DRAG OF FREE-FALLING SPHERES IN WATER FOR REYNOLDS NUMBERS NEAR CRITICAL

by

George Fred Nolan

United States
Naval Postgraduate School

THESIS

DRAG OF FREE-FALLING SPHERES IN WATER

FOR REYNOLDS NUMBERS NEAR CRITICAL

by

George Fred Nolan

September 1970

Drag of Free-Falling Spheres in Water

For Reynolds Numbers Near Critical

by

George Fred Nolan
Lieutenant, United States Navy
B.S., United States Naval Academy, 1963

Submitted in partial fulfillment of the
requirements for the degree of

MASTER OF SCIENCE IN PHYSICS

from the

NAVAL POSTGRADUATE SCHOOL
September 1970

ABSTRACT

Drag coefficients of free-falling spheres in water were determined in a 12-ft diameter tank. Nine spheres with weights ranging from 361 grams to 4587 grams were released from rest and their speeds measured 19.5 feet below the release point using orthonormal cinematography. The region on both sides of the critical Reynolds number was covered with Reynolds numbers ranging from 10^5 to 7×10^5. Spheres with Reynolds numbers less than the critical value displayed little scatter in their terminal velocities. The same was true for the heaviest sphere. However, spheres with Reynolds number immediately above the critical value frequently deviated from the normal trajectory and their speeds showed scatter as great as 20%. A plot of drag coefficient versus Reynolds number shows that free-falling spheres essentially conform to the wind tunnel results; the critical Reynolds number is unchanged and the drag coefficients differ no more than 20%, always being higher for the free-fall case.

TABLE OF CONTENTS

LIST OF TABLES

LIST OF DRAWINGS

LIST OF ABBREVIATIONS AND SYMBOLS

b	Radius of VAT
Cd	Drag Coefficient for Sphere
D	Diameter of Sphere
g	Acceleration due to Gravity
I	Image Distance of Lens
L_1	Distance from Lens to Air-Water Interface for Camera Number One
L_2	Distance from Lens to Air-Water Interface for Camera Number Two
m	Slope of Vertical Distance versus Frame Number
n	Index of Refraction
r	Radial Distance from Origin to Sphere on Film
R	Radial Distance from Origin to Sphere in Real Space, Correlation Factor
Re	Reynolds Number
U	Velocity of Sphere Relative to Fluid
VAT	Variable Atmospheric Tank
x,y,z	Coordinates of Sphere on Film
X,Y,Z	Coordinates of Sphere in Real Space
wppm	Weight Parts of Solute per Million Parts of Solvent
μ	Shear Viscosity
ν	Kinematic Viscosity
ρ	Density of Fluid
θ	Angle of Incidence
θ'	Angle of Refraction
ϕ	Angle Between Vertical and Sphere
1	Refers to Camera Number One
2	Refers to Camera Number Two

ACKNOWLEDGEMENT

First and foremost, to my wife, Bonnie, my heartfelt thanks for the understanding and devotion that was always present throughout this endeavor. To Professor James V. Sanders, my sincere graditude for the long hours and guiding hand that went beyond the normal role of Thesis Advisor. Particular thanks to the Naval Underwater Research and Development Center, Pasadena for permission to use the VAT and associated equipment and especially to Dr. Jack Hoyt. Also to Mr. Herman Torkelson my appreciation for the assistance and special efforts displayed in the lab and assembling needed equipment. Finally to LCDR John Kinnier my thanks for his advice and experience that was given freely in carrying out this experiment.

I. INTRODUCTION

A. DRAG REDUCING ADDITIVES

In 1948, Toms [30] reported that adding a high molecular-weight polymer to a solvent could reduce the drag experienced in pipe flow. Since he was the first to correlate the concentration of these additives to the amount of drag reduction (actually increased flow rates), subsequent authors referred to this effect as the "Toms Phenomenon." Early investigations showed that the amount of drag reduction was a strong function of concentration and, depending on the type additive employed, concentrations on the order of ten to one hundred parts per million by weight (wppm) achieved the best results. The polymers that are the best drag reducers were shown to possess a linear molecular structure and that there is a direct relation between the molecular length and the drag reducing capabilities. At a given concentration, the greater the molecular length of the polymer ingredient, the greater the drag reduction.

Hoyt and Fabula [13] used a rotating disk in polymer solution to show that drag reduction occurs only when the flow is turbulent. In pipes, flow must also be turbulent in order to experience drag reduction and in addition the shear stress at the wall of the pipe must exceed a critical value [15]. Experiments have also shown that degradation of the polymer additive will occur in turbulent flow, thus altering the drag-reducing behavior.

1. Applications

With little thought, a wide variety of applications can be imagined for these flow "lubricants." To date, polymers have been employed in sewage systems to increase flow rates, thus averting costly expansion

projects. Transportation of crude oil from the fields via pipes require huge pumps. Thus oil companies are interested in reducing the size and power of these pumps by using suitable polymers. Various fire departments have succeeded in obtaining high velocity streams of water (longer streams of water) from existing equipment. Persons suffering from high blood pressure and weak hearts may some day obtain relief with an intervenous injection of a physiological compatible polymer additive. The Navy and Merchant Marine are highly intrigued in the development of these water soluble lubricants to reduce the power (fuel) required to propel large ships through the water. At present, this is economically unfeasible for it has been estimated that for a 450 foot vessel traveling at eighteen knots, it would require 1800 pounds of polymers additives per minute. But for small bodies with limited range, such as torpedoes, practical applications are already at hand. Limited success has been demonstrated with smaller waterborne craft to the extent that International Yatch Racing Rules specifically state that it is illegal to use any type of these drag reducing additives to reduce the drag of water moving along the ships hull.

2. Mechanism

Science has shown that once the mechanism of a particular process is known it can usually be employed in a more efficient manner. This particularly applies to the study of long-chain macromolecules that exhibit drag-reducing properties. Such study should also improve our insight into the physics of fluids.

B. EXPERIMENTAL FACILITIES

Experiments designed to determine the specific properties of polymers basically fit into two categories: pipe flow and flow about finite bodies.

Pipe flow is characterized by drag due to skin friction. It has the advantages of using premixed, homogeneous solutions where the entire mixture undergoes more or less the same process. Only small quantities of polymers are used. Measurements consist of determining the pressure gradient and flow rates to fix the Reynolds number (Re) and drag coefficient (Cd). Another aspect of pipe flow is that, for the laminar flow of a Newtonian fluid, the solution to Navier-Stokes equation agrees with experimental data. Even when the flow is turbulent, well defined semi-empirical relations exist for Newtonian fluids such as water. Thus, there are agreed upon standards with which to compare results obtained with polymer solutions in pipe flow. The greatest disadvantage is that the turbulence causes degradation (breaking up of the macromolecules) which might make data interpretation difficult.

Bodies of finite size such as disks and cylinders can be rotated in premixed, homogeneous polymer solutions and meaningful data is obtained by monitoring the torque required to drive the body. Drag is again due to skin friction. Other types of experimental facilities used with finite bodies are the wind or water tunnel where the fluid is moved by a fixed body. The reversal of this situation is a towing tank. Facilities that use only gravity as a means of achieving acceleration are termed free fall. Finally, the body may be self-propelled. All the above methods have their advantages and disadvantages and the selection is dependent on what are the desired results in the way of data and the particular logistics associated with the experiment.

C. FLOW ABOUT SUBMERGED BODIES

At high Reynolds numbers submerged bodies are described as either streamline or blunt. For a streamline body, the wake is very small and the drag is predominately due to skin friction. For blunt bodies, the wake drag exceeds that due to skin friction.

1. Flow about a Submerged Sphere

To describe the flow about a sphere in an Newtonian fluid it is often sufficient to specify the drag coefficient (Cd) which is the drag force divided by the dynamic pressure ($1/2\ \rho U^2$) and cross sectional area ($\pi D^2/4$) of the sphere, and the Reynolds number (Re), which is the relative speed (U) between the fluid and the sphere times the diameter of the sphere divided by the kinematic viscosity (ν). For Reynolds numbers less than unity there exists a closed form solution to the Navier-Stokes equation that has neglected inertial forces. Experiments have born out its validity. In this region flow is laminar and well behaved. For Re > 1, there are no known closed form solutions and the resulting differential equation has only numerical solutions. At about Re = 17, separation takes place and a wake begins to form. Above Re = 40 only experimental results are available. At Re = 140 vortices form in the wake alternating from side to side. The Re vs Cd curve flattens out at about Re = 10^3 and the flow is characterized by a fully developed wake. The wake is a turbulent region bordered by a laminar boundary which leaves the sphere just before the equator. At Re = 2.5×10^5 there is a marked decrease in wake size and the Cd also takes a sharp drop. This region is commonly referred to as the critical region. Several theories exist to explain this sudden decrease in wake size. The more generally quoted hypothesis is that the laminar boundary layer becomes turbulent before separation. Since a turbulent boundary layer can support a larger adverse pressure gradient before separation occurs, the wake diameter is decreased. But Roshko [26] has observed for cylinders that after the sharp drop in Cd, the curve immediately begins to rise and then flattens out at a value of Cd below that existing before the critical Re. He

proposes that a "separation bubble" is formed and that the transition to the second plateau is due to the disappearance of this bubble. Sanders [27] postulates that this separation bubble theory is also applicable to spheres.

Standardization of the drag coefficient curve for spheres was achieved in the twenties and early thirties primarily due to the efforts of individuals like Wieselsberger [36], Jacobs [14], Bacon and Reid [1], Millikan and Klein [21], and Flachsbart [7]. This curve can be divided into four parts: (1) Stokes Law Region, $Re < 1$, (2) Transition Region, $1 < Re < 10^3$, (3) Newtonian Region, $10^3 < Re < 10^5$, and (4) the Critical Region, $Re > 10^5$.

Lunnon [17] in 1926 made a series of drops with spheres down mine shafts and also in water [18] and was able to confirm the wind tunnel results up to $Re = 10^4$, but when these results approached the critical region the free fall results differed considerably. Goldstein [9] illustrates these differences on page 495. Also included on this graph are the free-fall results of Bacon and Reid [1] for Reynolds numbers above critical which further points up this discrepancy. This difference in results between free fall and wind tunnel continued to exist without confirmation or justification. The subject laid dormant until Barker [3] in 1951, studying the free fall of various shapes, empirically determined correction factors that would bring both his and Lunnon's data in agreement with the standard Cd vs Re curve of the wind tunnel. Barker worked in the Newtonian range. He was the first to report that spheres in free fall deviated from the true vertical in a rather random fashion. He did not take this deviation into consideration when computing drag coefficients, but did state that for this reason, free-fall results should not be compared to those of the wind tunnel.

Barker's work is a typical example of the type of progress made in fluid dynamics since the advent of the wind tunnel; individuals applying empirically determined modifications to existing theory. The mathematics are so involved that even todays computers have had limited success in solving the Navier-Stokes equation for Re > 1.

2. Free-Falling Spheres in Polymer Solutions

The interest in polymer drag reduction has rejuvenated an interest in this field of fluid dynamics. Sanders [27] outlines the history of experiments with spheres in polymer solutions and summarizes the results. His article was based in part on the data obtained by Hayes [10] who worked in the Transition and Newtonian range ($0.8 \times 10^3 < Re < 7 \times 10^4$). Basically the results were that when flow is characterized by a fully developed wake, significant drag reduction is obtained only with the same polymers that are known to reduce turbulent skin friction. Also maximum drag reduction is achieved using minute amounts of polymers. He therefore attributes the drag reduction to the same mechanism, and postulates that the polymers reduce the diameter of the wake by delaying the separation of the laminar boundary layer. This hypothesis is supported by photographs obtained by Patrick and Lang [16].

Woolery [37], continuing the work of Hayes, investigated the Critical Region. He used an injection technique that placed the sphere in motion at or near its terminal velocity. The velocity was obtained using horizontal planes of light equally spaced which the sphere interrupted as it passed. Thus he was restricted to only the vertical component of velocity and could comment only qualitatively on the horizontal component of the sphere's trajectory. Woolery obtained evidence of drag reduction above the critical Reynolds number (2.5×10^5) but could not

confirm the amount due to the uncertainty in the standard curve. His results in water compared favorably to the wind tunnel curve. But if the results of Bacon and Reid are correct for freely falling spheres, then there must be something wrong with Woolery's experimental procedure and all of his results would be thrown into doubt.

Thus there appears to be a need to confirm this region of interest. Lang and Patrick in their work with polymers also stated that valid measurements were required in this area.

II. METHOD

A. EXPERIMENTAL TECHNIQUES

Once it was decided that more data were required on freely falling spheres in Newtonian fluids near the critical Reynolds number, it was then a question of how to obtain these data.

There are few experimental procedures available from which to select a suitable method to obtain data on a truly free-falling sphere in the Critical Region. First, the experiment is restricted to either air or water as a fluid medium. They are the only fluids available in economically feasible quantities that have low enough kinematic viscosity to allow objects to reach the high Re required and still keep the size and density of the sphere within reasonable limits.

In air it is estimated that the height required to obtain terminal velocity (point where the buoyant force plus the drag force equals the gravitational force) is between 200 and 300 feet for this range of Re. This height precludes any "laboratory" facility and thus the experiment must be taken into the field where nature becomes a contributing factor. Lunnon used mine shafts, Bacon and Reid used airplanes and Barker attempted to use an abandon chimney to achieve sufficient fall distance. Each were faced with problems such as varying wind currents, documentation, and temperature gradients that would not ordinarily be critical factors in a laboratory environment. In water, things appear to be a bit easier since water depths of only eighteen to twenty feet are required to achieve terminal velocity.

Devices to measure speed are limited to extrinsic devices if the sphere is to be truly in free fall. Early methods used to obtain data were strobe photography, crude chronographs, and theodolites. More

sophisticated methods have been developed including a unique procedure employed by Pasternak [24]. Using a nuclear reactor, he irradiated his objects to produce radioactive isotopes that had half-lives of four to five days. He then used an array of Geiger counters to sense the passage of his objects in free fall. Other techniques are discussed by Torobin and Gauvin [31-35] as well as Woolery [37]. No further details will be given except for the methods actually attempted.

B. SELECTION OF METHOD

The first attempt to develop an experimental technique with which to determine the terminal velocity of gravity-driven spheres incorporated the use of a helicopter and a chronograph radar. It seemed a simple matter to gain the desired altitude with the aid of the helicopter and with the proper employment of the chronograph to determine the sphere's velocity. The chronograph selected was an Army AN/GPS-5 which uses the Doppler principle to compute velocity. This particular instrument gave a digital readout of velocity to the nearest tenth of a meter per second. Since the chronograph was originally designed to give a single reading (actually muzzle velocity of a projectile fired from heavy artillery) a slight circuit modification would be necessary to give continuous readings as the sphere descended. This is necessary to determine if the sphere had in fact reached terminal velocity. The rub lay in that the chronograph could not be made available at the required time, therefore this method had to be discontinued, but it still appears to be an excellent method.

Next in the search for a suitable method was the decision to try the same principle as the chronograph but the medium would be water and the signal source sonar. The difficulty here was that any echo from a solid sphere would be at best thirty decibels down depending on signal

wavelength to sphere diameter ratio [8]. Thus a variable signal source was required as well as a variable receiver with highly discriminatory features. The logistics of the experiment also seemed to be enormous. One would have to perform the experiment in deep water to reduce unwanted reverberations and an area of little or no ambient noise was needed. Additional considerations of support for the operation with power, equipment, and sphere recovery techniques caused this method to be rejected.

Photography was the next method investigated. Experimentation with strobe photography was initiated using the same cylindrical tank employed by Woolery. At first, only one camera (Graflex Speed Graphic) was used, but in order to obtain more information about the trajectory of the sphere two cameras, orthonormal to one another, were employed. This would allow the horizontal velocity to be determined. The inside of the tank was painted flat black which was a mistake since a white background gave better contrast. A two inch aluminum sphere was chosen as the test object. When ordinary tap water was used it was found that it had to be filtered in order to avoid the adverse effect of light back scatter which quickly over exposed the film. Filtering was accomplished by a simple fiberglass filter made by stuffing odd shaped pieces of fiberglass into an open-ended length of tubing. This allowed a higher f/stop to be used thus increasing both the time the camera could be left open and the depth of field. With the strobe light directly over head and the camera's shutter open for one second of the fall, a multiple exposured film was achieved. Measuring the distance between sphere images and knowing the frequency of the strobe light, the velocity was determined using a simple geometric relationship.

After this technique was mastered it was determined that high speed motion pictures cameras could be made available. Believing that better information could be obtained with less chance of missing the sphere in a given drop, the conversion to cinematography was made.

III. EXPERIMENTAL PROCEDURE

A. VARIABLE ATMOSPHERE TANK

The Variable Atmosphere Tank (VAT) at the Naval Underwater Research and Development Center, Pasadena, California, was used as the test site. The VAT was originally constructed to test models of the Polaris missile underwater launching system and the primary method of data taking was cinematography. Thus the VAT appeared to have all the features necessary for the free fall experiment. A physical description of the VAT is contained in Appendix A.

B. CAMERAS

For data taking, two Mitchell GC 35mm high-speed motion picture cameras were positioned to give orthonormal viewing of the falling sphere. Figure 36 shows their respective positions. This type of camera is widely employed by the Navy at test sites located at Morris Dam and San Clemente Island. The film frame rate was set for seventy-five frames per second with maximum film rate available of 128 frames per second. The film rate can not be assumed as constant and to insure timing accuracy the camera has incorporated an electronic timing network that triggers a neon light that is set to expose the outer edge of the film. This timing network was set for one mark every one hundredth of a second. The two cameras were not synchronized frame for frame, but this appeared to be no problem since the film frame could be matched to within a frame by spatial coordination.

Besides the 35mm cameras, a Photosonic 1B 16mm high-speed motion picture camera was used for documentation purposes. It was positioned approximately seven feet directly above the release mechanism to give

a vertical view of the falling sphere. Figure 3 show this set up. The overhead camera's purpose was to record each drop as to initial trajectory and rotation of the sphere, as well as detect any spin imparted to the sphere by the releasing mechanism. It was not anticipated that measurements would be taken from the 16mm film, therefore no timing mechanism was used with the overhead camera although the film frame rate for this particular camera is very accurate. The film frame rate was set at one hundred frames per second. It was not expected that the total trajectory of the sphere would be observed by the overhead camera even if the trajectory of the sphere was truly vertical. The depth of field of a camera through an air-water interface is very poor.

Kodak Ektachrome, film type 5242, was used in the 35mm (data recording) and black and white Eastman 4X, type 7224, was used with the 16mm (documentary) camera. This film combination was dictated by local logistics. Seventy millimeter film or larger would have been preferred over the 35mm for data taking purposes.

C. SPHERES

Nine spheres were chosen to cover the range of Reynolds numbers in the critical region. The physical characteristics are shown in Table I. These are the same spheres used by Woolery [37] in his work on drag reduction. At the recommendation of the photographer, the spheres were painted with orange lacquer in order to give the best contrast when photographed with color film against a white background. The thickness of the paint and its added weight would appear to affect the terminal velocity but Barker reported that a slight coat of paint effected the terminal velocity of his non-isometric shapes very little.

After the paint was applied, the spheres were then numbered in order of decreasing Reynolds number. Scribe marks were placed about the numbers as shown in Fig. 1. The purpose of these scribe marks was to facilitate observation of spin if any existed. It was not the objective of this experiment to determine spin in a qualitative fashion. Using an ordinary brand of car paste wax, the spheres were then polished to give a uniform smoothness.

D. RELEASE MECHANISM

The objective in the design of the sphere release mechanism was to place the sphere into free-fall motion with little or no velocity, translational or rotational. Secondly, there existed the requirement that the medium into which the sphere was being released be disturbed as little as possible by the operation of the device. The final product is pictured in Fig. 2. The device is electromagnetic in nature, releasing the sphere when the current to the magnet is interrupted. The power source was an ordinary 115 VAC household outlet. The mechanism was completely submerged along with the sphere when released. Adapters plates were attached to the underside of the release mechanism to accommodate the four different diameters of the nine spheres. See Fig. 2.

E. REFERENCE MARKS

The thirty-five millimeter cameras were aligned to reference marks that were surveyed into the VAT. A portion of the left side of the VAT and its reference marks are illustrated in Fig. 37. This alignment insured that the optical axes of both cameras were in the same horizontal plane as well as separated by an angle of ninety degrees. The blueprint from which Fig. 37 was taken quoted the tolerances of the reference marks to be within $\pm$ .00015 inches.

F. DROP PROCEDURES

The release mechanism was attached to a seven foot aluminum pole which was in turn fastened to the tip of an overhead monorail which could be run in and out of the VAT through a water tight hatch. See Fig. 3. The spheres were placed in the release mechanism and then the monorail was run out until it placed the releasing mechanism with the sphere approximately in the center of the VAT. The depth of the water from the underside of the release mechanism to the horizontal plane of the 35mm camera's optical axes was approximately 19.5 feet. It was theoretically predicted that it would take eighteen feet of free fall for the largest of the nine spheres to reach 98% of its theoretical terminal velocity. See Hayes [10]. The cameras were started just prior to releasing the sphere by a remote interrupt switch. The time between drops was more then sufficient to allow the disturbances caused by the preceeding drop to be damped out. Also the sphere was entirely submerged when released thereby avoiding bubble capture which would upset the flow characteristics. Once all nine spheres were dropped, which constituted a run, the platform was raised to retrieve the spheres. This raising of the platform caused considerable disturbances in the water, therefore at least an hour was allowed between each run. The smallest VAT diameter to sphere diameter ratio was 36 and according to McNown, et al., [20] and Fidleris and Whitmore [6] wall effects can be ignored. If the sphere hit the side of the tank the drop was disregarded. In about one out of every five drops this did occur. By inspection of the cross-sectional area of camera coverage shown in Fig. 36 it can be seen that the sphere must be in the general proximity of the center of the VAT if it is to be photographed by both cameras. This figure does

not take into account refaction. If both cameras did not pick up the sphere, the run was disregarded. The platform was covered with two-inch thick "horsehair" matting to cushion the fall of the spheres. This worked well except for spheres one and two. They received healthy dents on several drops. After each run, they were inspected for damage and then rewaxed. Any damage was repaired before the next run. In runs four and five, sphere number one had defect that made it marginal as far as its dynamic characteristics were concerned.

IV. DISCUSSION OF RESULTS

A. LESSONS LEARNED

Since this paper deals with not only verification of data in the critical region, but also development of an experimental technique with which to measure these data, it would be well to discuss mistakes and lessons learned in obtaining and reducing data.

1. Equipment

The data recording cameras used were reliable ones, but they were first put into production in 1928 and with minor modifications have had continuous services for the past forty-two years. There exists more modern cameras with features such as constant film speed, integrated timing network, and film frame synchronization.

Since timing appeared to be the ultimate limitation in data reduction, it would be well to continuously monitor the timing mechanism with a frequency counter instead of just periodic checks. Binary timing could also be employed which records on the film total elapsed film time in a binary code that can be read directly.

The 16mm documentary camera had little success in carrying out its function. Filming through an air-water interface is difficult if the water's surface is smooth and undisturbed, but with the slightness disturbance it becomes impossible. The releasing mechanism although designed to cause as little turbulence as possible, still propagated surface ripples when actuated. These ripples completely obscured the trajectory of the falling sphere. Thus nothing was gained from this camera, quantitative or qualitative. If an overhead camera is used, it must be mounted below the surface or have an intermediate translucent

interface at the surface to eliminate any ripples. Also underwater lights should be used to reduce the light reflection from the water's surface.

The markings on the spheres were not visible from either of the 35mm or the 16mm cameras. Possibly just by making the markings large and darker could correct this situation.

2. Alignment

In order to use simple data reducing techniques, it is imperative that the cameras be orthonormal and to further simplify the reduction, the lens of the two camera should be equidistant from the center of the tank. Also it would aid in data reduction to have visible to both cameras an object (meter stick mounted vertically) that is a known distance from both cameras. This is not mandatory, but is a good procedure and can be easily accomplished using the center of the VAT platform to mount the meter stick, length of straight tubing (pipe), etc., in the vertical axis of the VAT.

3. Procedure

The only modification to the procedure would be to have the camera man maintain a log on the camera's running time. This correlated with the sphere drop log would make the editing of the film a less complicated process.

B. DATA REDUCTION

1. Film Readings

The film was edited using a 35mm viewer. Here is where a camera operating log would have been beneficial since both cameras did not pick up the sphere all the time and sometimes the cameras were turned on for testing purposes, therefore not all the blank film could be attributed to missed opportunities. The film strips were

compared, matched and documented as to run, drop, sphere, and camera number. The majority of the film strips were sent to Pt. Mugu, California, where they were processed by a comparator, trade name "Telereadex." The Telereadex automatically records the location of the origin (reference mark) on the film frame, thus only one marking is necessary per film frame, that is, only the location of the sphere must be pointed out at the machine which will then record the run, drop, sphere, and camera plus the film frame number and then reads out the x-y position of the sphere in machine units. These machine units were converted to distance on film in centimeters. It took approximately three hours to process all the film strips. Frame numbering commenced with frame in which the sphere first begins to appear.

Three drops were processed by hand using a table comparator. This method took about one hour per drop.

2. Data Analysis

The readings obtained from the film (z_1,y) from camera number one and (z_2,x) from camera number two, were converted to real space (X, Y, Z_1, Z_2) using the thin lense approximation. The origin was taken as the center of the tank. Refraction was taken into consideration using Snell's Law. An index of refraction of 1.000 was used for air and for water 1.333. The basic relations are shown in Fig. 4 and 5. The mathematics and computer programs are contained in Appendix B. The programs shown are written for the Hewitt Packard 9100A computer. Programs A and B were used to reduce data to spatial coordinates. Program C is a Linear Regression and Correlation Factor routine. Programs A and B are actually one continuous program but due to the limited memory of the 9100A, the routine was divided into two programs.

The vertical position (Z_1 and Z_2) versus frame division were plotted. A frame division can vary as to the amount of time it represents. For a slow moving sphere it can incorporate as many as five film frames whereas for the faster moving spheres it may be as few as one. This method was used to avoid needless calculations and still give a representative picture of the entire photographed drop. Ideally this plot should be two straight lines superimposed on one another. Two contributing factors caused this not to be the case. First, the film speed of the cameras were not the same for a majority of the drops. Secondly, there is a fractional frame separation between frames of the respective cameras. They are only in phase when the lines intersect. If the lines are not straight then the sphere is accelerating or the film speed is not constant. The latter was definitely the cause in two cases where the lines were not straight and this was corrected for in a manner to be described later.

Figures 6 through 33 shows the vertical position versus frame number plots. Included in these figures are plots of the horizontal trajectories of the sphere for the same time period. The scales for both plots are the same except where indicated.

The vertical distance versus frame number for each drop was entered into Program C. The correlation factor (R) is an indication of the straightness of the lines with unity being a perfect straight line. Correlation factors greater than 0.9999 were achieved in most cases. The slope (m) was obtained from Program C, too, Time (t) indicated in the figure is actually time per frame division which was measured directly from the film using a table comparator. If this time were not constant, i.e., the camera was not running at a constant speed,

then a plot was made of film distance versus timing marks thus obtaining an instantaneous time for each frame division, then the procedure outlined below was used.

The procedure used if the cameras were not up to speed when filming the sphere (film frame rate accelerating) are illustrated in figures 14, 15, 16, 18, 19, and 20. First a vertical position versus frame number was plotted as above (Figs. 14 and 18). Then the film distance versus timing marks were plotted (Figs. 15 and 19). Also indicated on the graph is the center of each film frame. The film frame centers were advanced fifteen frames to allow for the time lag between when the film is exposed and when the timing mark is inscribed. These two graphs are then superimposed using frame numbers to coordinate the transformation of vertical position and elapsed time (Fig. 16 and 20). The slope of this line is the vertical velocity of the sphere (U).

C. ERROR ANALYSIS

1. Random Error

Random error due to measurements is averaged out using the linear regression routine and can be represented by a portion of the difference in the two vertical velocities. The error in time was reduced by averaging it out over the entire drop. No quantitative measurement can be made except to include it as part of the percent difference in the vertical velocities.

2. System Errors

The only error that was allowed to stand without attempted correction was that introduced by the optical axis differing from the geometric axis (diameter) by approximately five degrees. This created a maximum error of four percent when the sphere was at the periphery of the film to zero at the center.

Another approximation was that $x_1 = x_2$ and $y_1 = y_2$. No calculations were made as to the effect of this approximation.

D. RESULTS

The proof that the assumptions and approximations are valid is born out in the results. Spheres six, seven, eight, and nine lie along that portion of the Cd curve that is well defined and agrees with existing data. Therefore it can be assumed that the results for the remaining spheres are equally valid to within that difference that their vertical velocities match for a given drop. Plotted in Fig. 34 are the results. Calculations for Re used a value of .088 poise for kinematic viscosity corresponding to a water temperature of 79.5°F. Also plotted in this figure are Woolery's results.

E. HORIZONTAL TRAJECTORIES

As mentioned earlier, the horizontal motion of the sphere is plotted in figures 6 through 33. It can be noted that in some cases the horizontal motion could contribute greatly to the overall translational velocity and in other cases not at all. The X-Y coordinates were plotted mainly for comparison purposes. Some figures show that the sphere is truly spiralling and some have no apparent physical significance.

V. CONCLUSION

A. COMMENTS ON EXPERIMENT

For work of this type the Variable Atmosphere Tank at the Naval Underwater Research and Development Center, Pasadena is a very useful tool. Camera coverage is available throughout the tank. Air-water entry under variable pressures can be studied. It is possible to add polymers in controlled concentrations for drag reduction work.

The cinematography aspect of the experiment worked out very nicely, and with the minor adjustments and alterations discussed earlier, the results can be even better. It is an excellent method for studying the total motion of a body which is important in an unconstrained, three dimensional, motion of free-falling objects like spheres. If the entire trajectory can be observed and recorded for analysis, it may be possible to explain why the sphere sometimes spirals and why it sometimes takes up a random, erratic trajectory.

B. DRAG COEFFICIENT OF FREE-FALLING SPHERES

The results of the present experiment are shown in figure 34 along with Woolery's. Evidently, for spheres eight, seven, and six, Woolery was able to "punch" through the "barrier" with his injection technique to achieve higher velocities than would ordinarily be observed in free-fall. Otherwise the results match fairly closely. Therefore, it can be assumed that his drag reducing data is also correct.

There is still some doubt as to how closely the free-fall data follows the wind tunnel curve and much more data should be taken to give some standard as was done in the wind tunnel experiments of the thirties.

TABLE I

PHYSICAL CHARACTERISTICS OF SPHERES

Sphere Number	Material	Diameter Centimeter	Mass Grams	Density $grms/cm^3$
1	Brass	10.1396	4587	8.288
2	Brass	8.8925	2918	7.925
3	Brass	7.6022	1824	7.928
4	Brass	6.3525	1131	8.426
5	Aluminum	10.1196	1502	2.768
6	Aluminum	8.8762	1018	2.780
7	Brass	5.0637	572	8.416
8	Aluminum	7.6245	645	2.779
9	Aluminum	6.3500	361	2.693

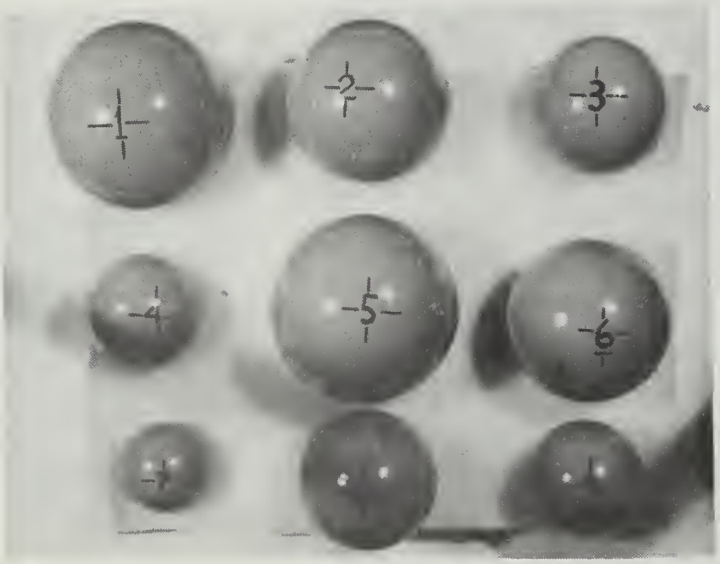

Figure 1. Nine spheres used in data taking. Sphere size range from 4 inches to 2 inches in diameter.

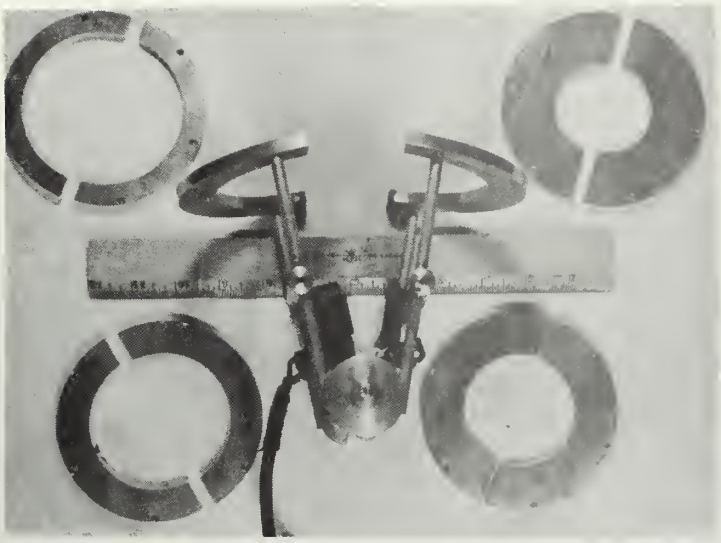

Figure 2. Release mechanism with its four adapter plates.

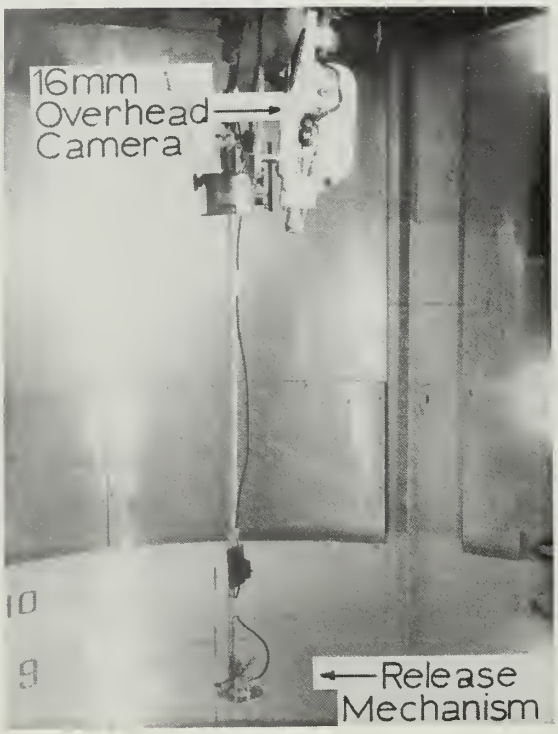

Figure 3. Experimental setup showing release mechanism with sphere in release position (approximately center of VAT). Release mechanism is totally submerged. Pole is attached to monorail which can be run in and out of VAT. Also shown is the 16mm documentary camera.

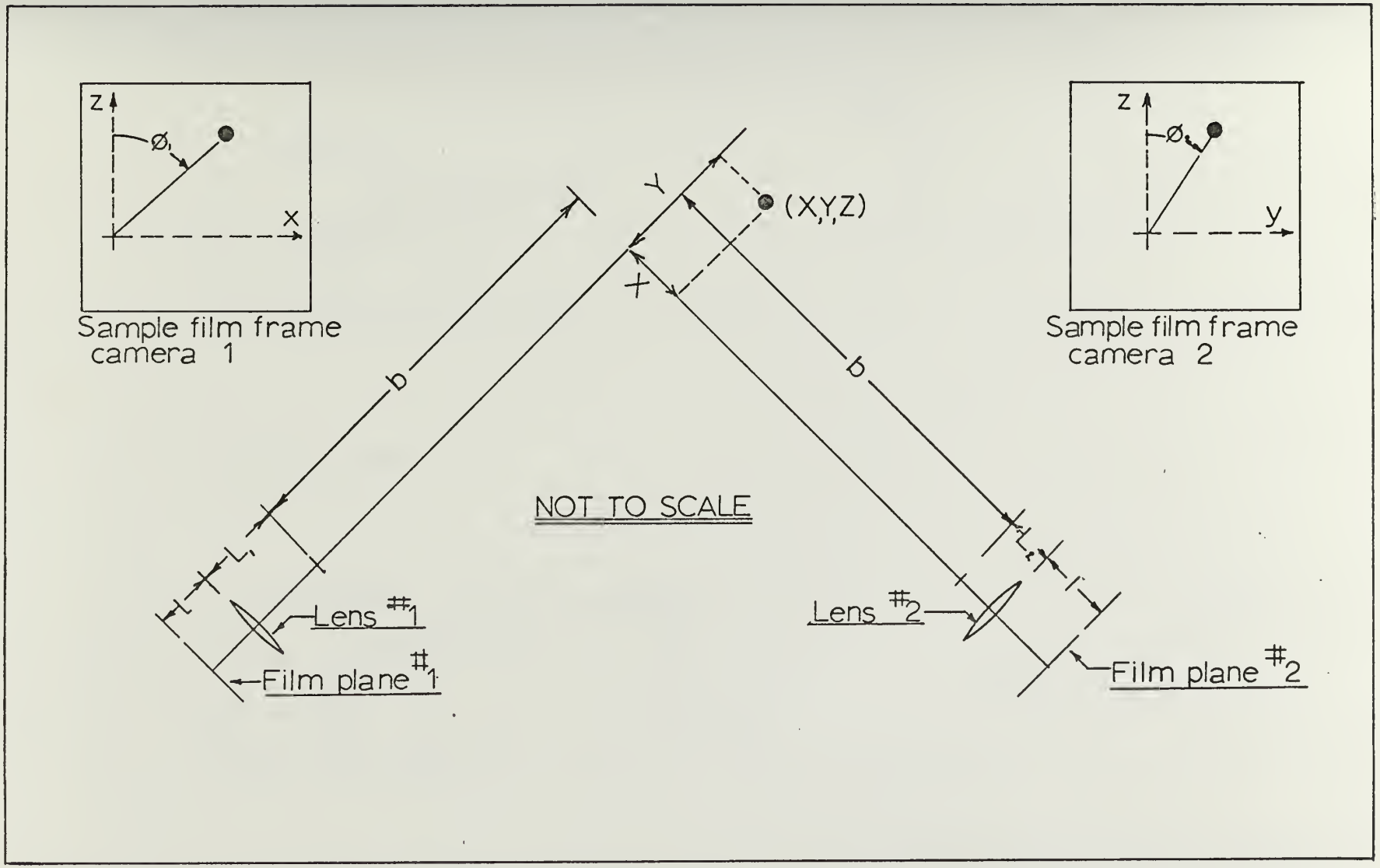

Figure 4. Shows orthonormal setup of cameras and defines parameters. Note that film position of sphere is denoted by (x,y,z) and real space is (X,Y,Z).

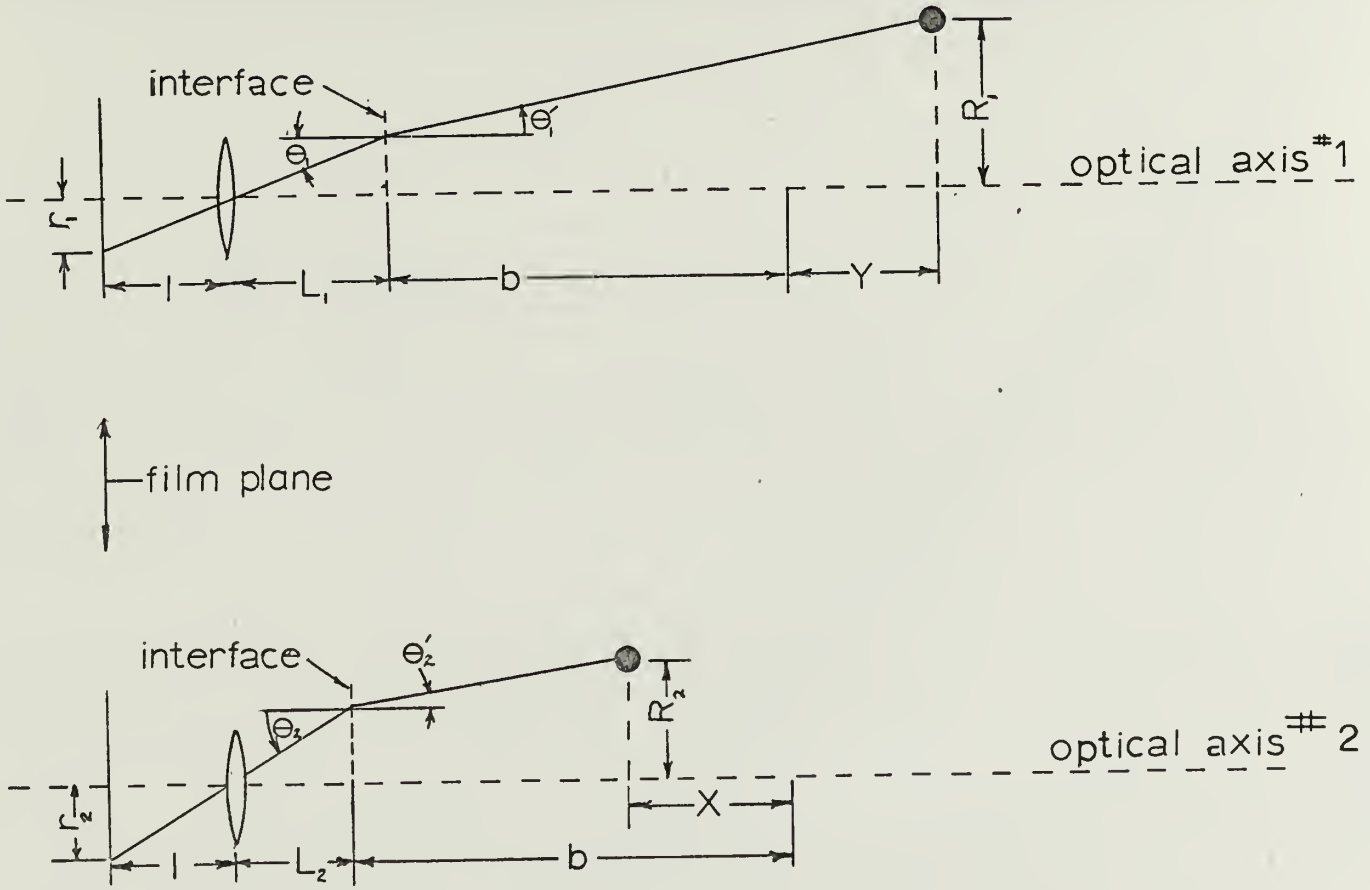

Figure 5. Geometry in plane of sphere and optical axis. Note that X is negative and Y is positive in the configuration.

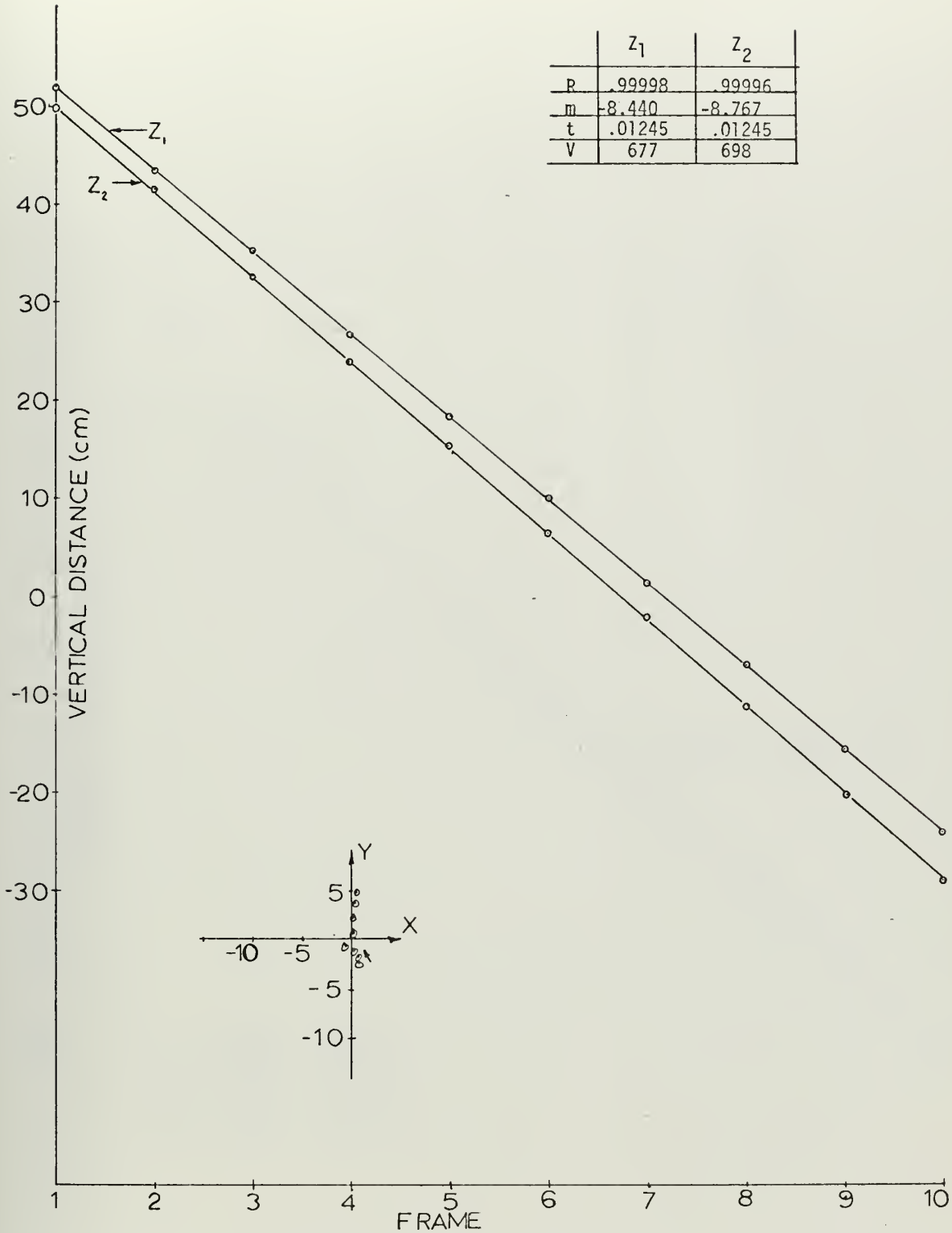

	Z_1	Z_2
R	.99998	.99996
m	-8.440	-8.767
t	.01245	.01245
V	677	698

Figure 6. Data Run #1 Sphere #1.

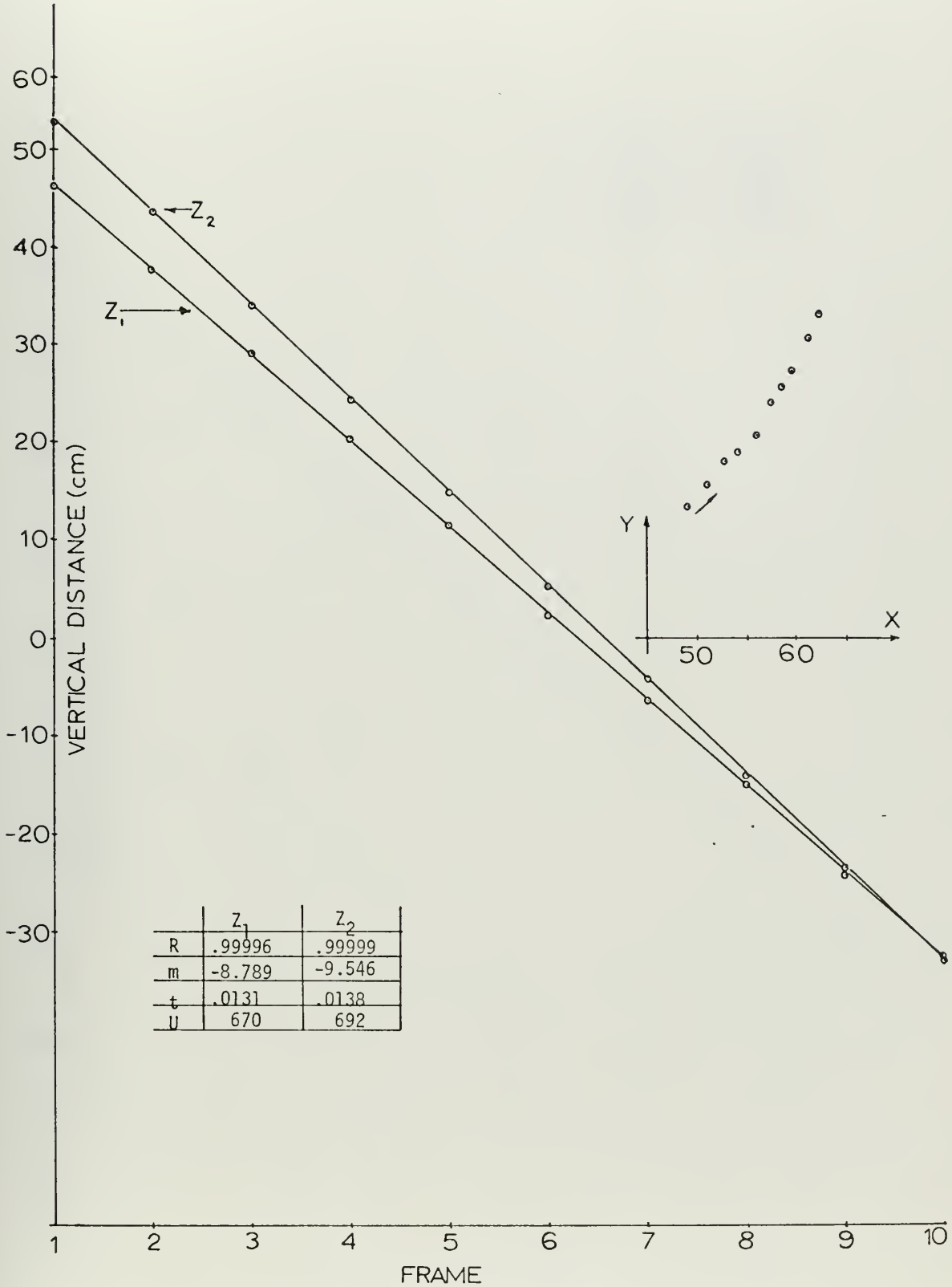

	Z_1	Z_2
R	.99996	.99999
m	-8.789	-9.546
t	.0131	.0138
U	670	692

Figure 7. Data Run #2 Sphere #1.

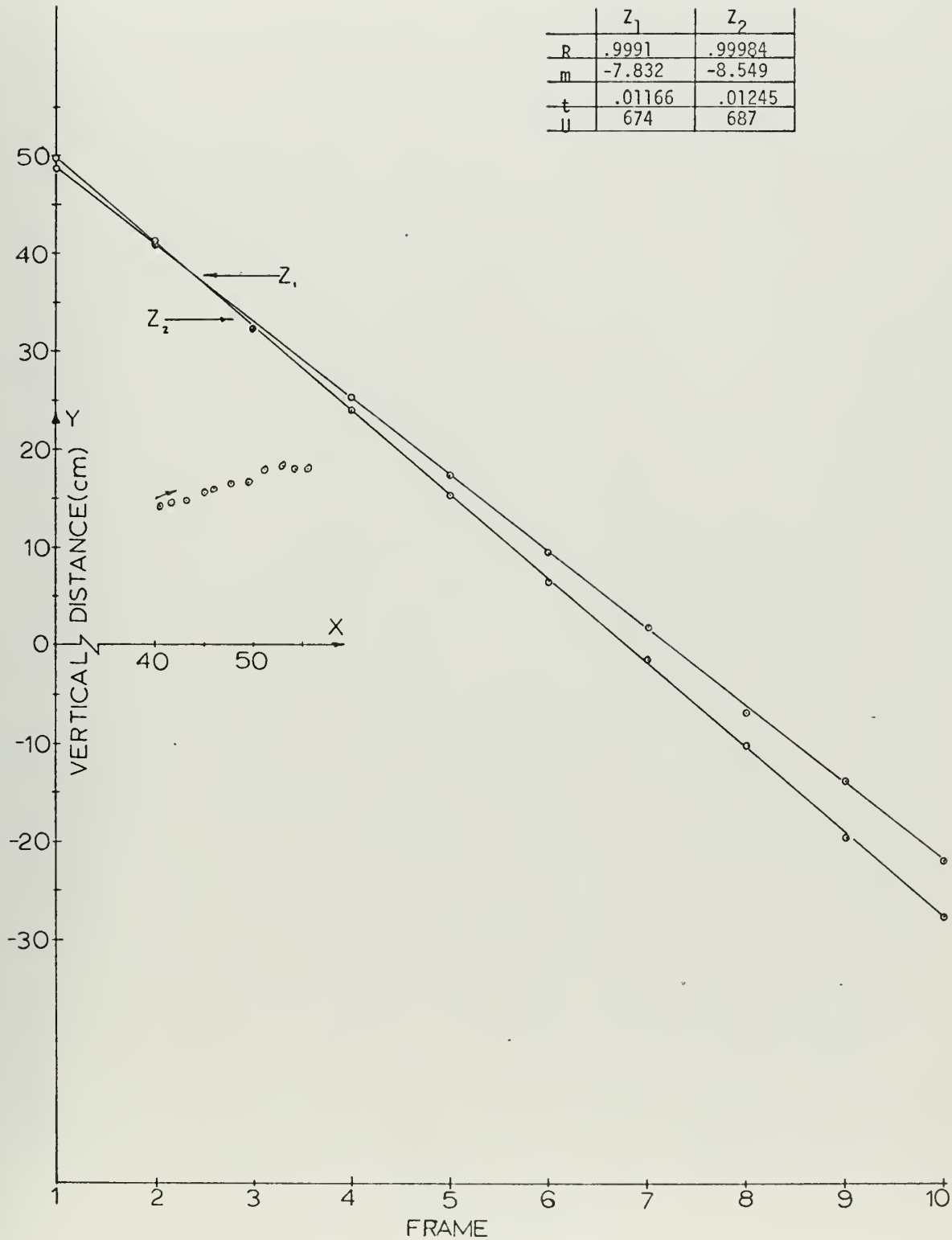

	Z_1	Z_2
R	.9991	.99984
m	-7.832	-8.549
t	.01166	.01245
u	674	687

Figure 8. Data Run #3 Sphere #1.

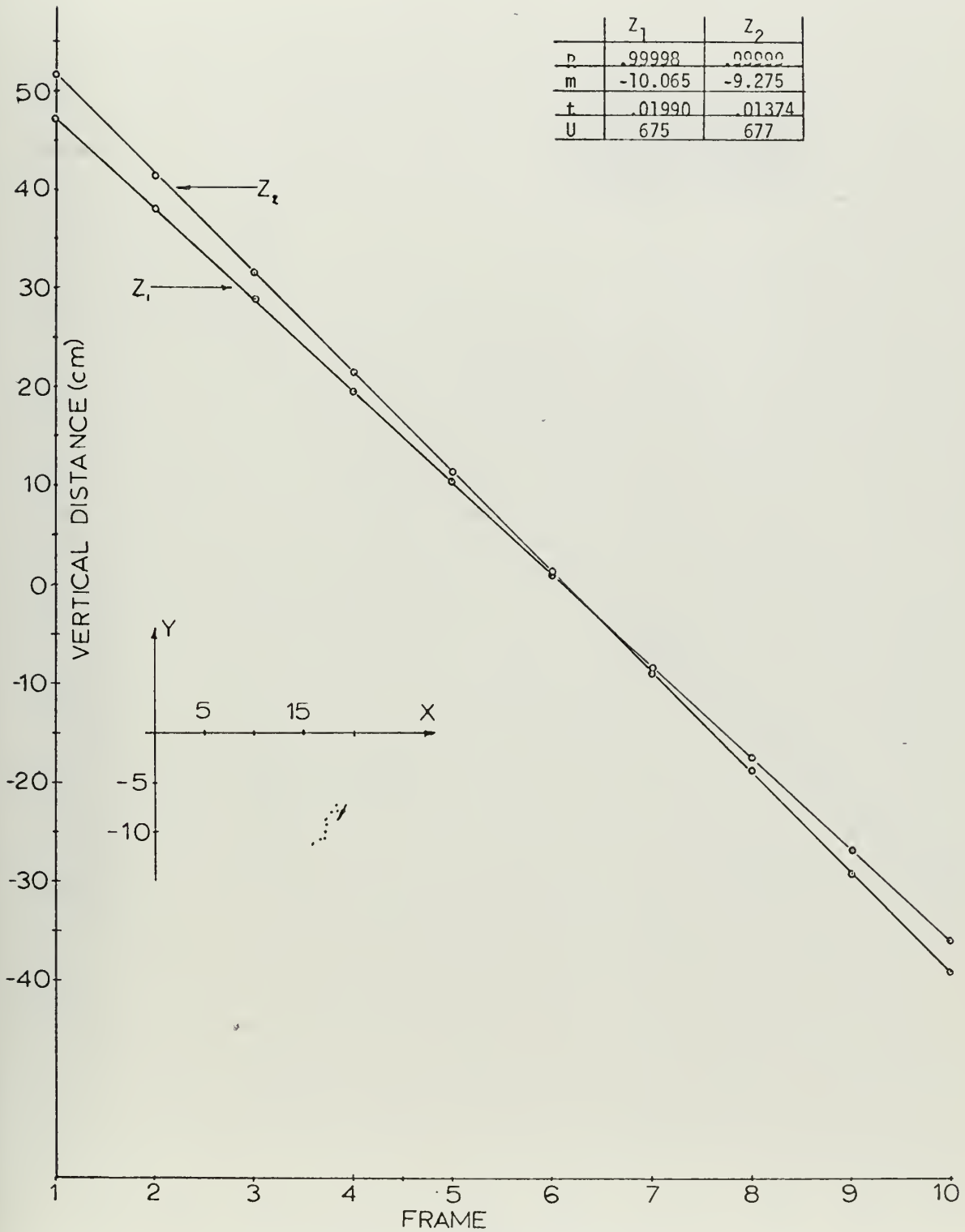

	Z_1	Z_2
p	.99998	.99999
m	-10.065	-9.275
t	.01990	.01374
U	675	677

Figure 9. Data Run #5 Sphere #1

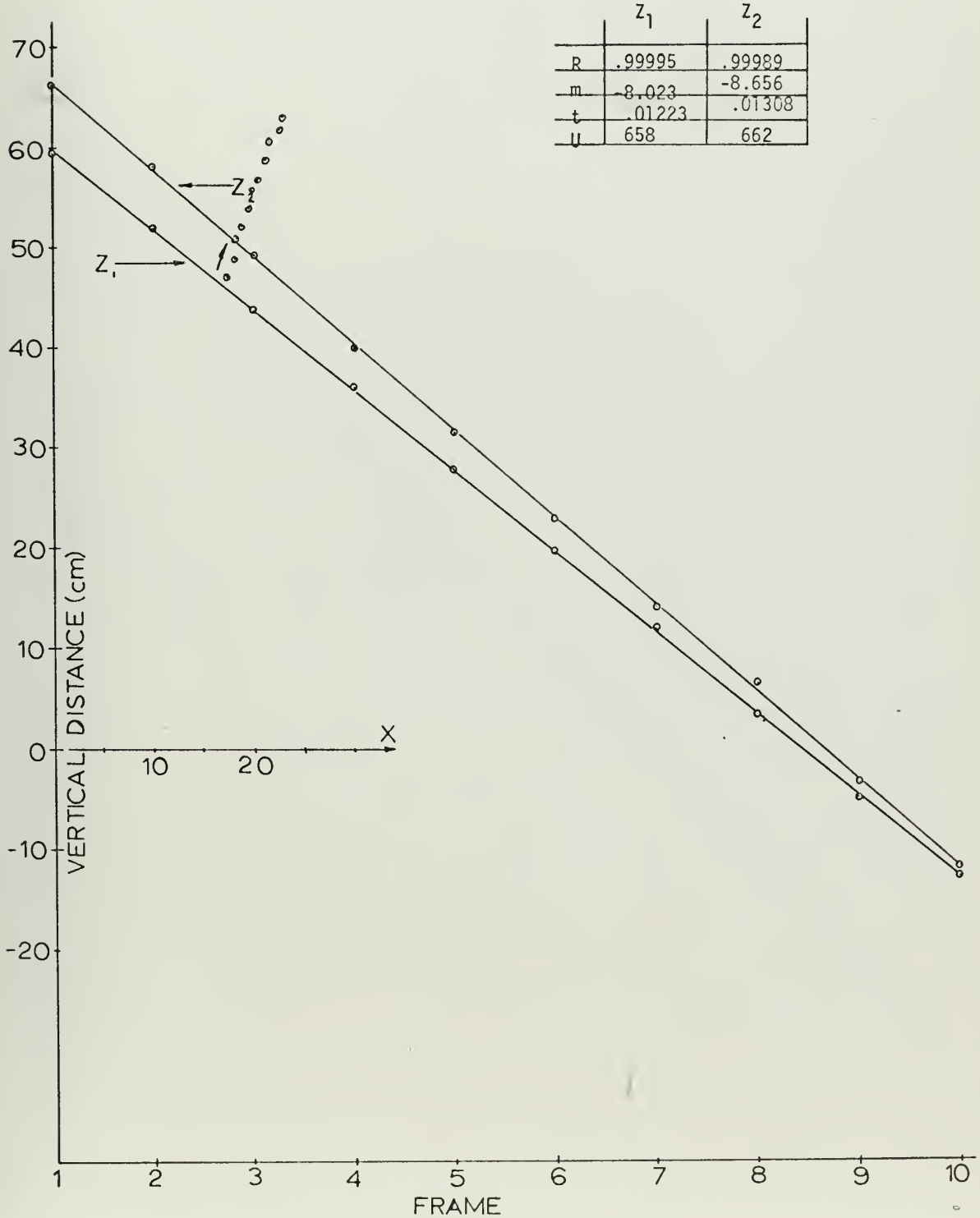

Figure 10. Data Run #3 Sphere #2.

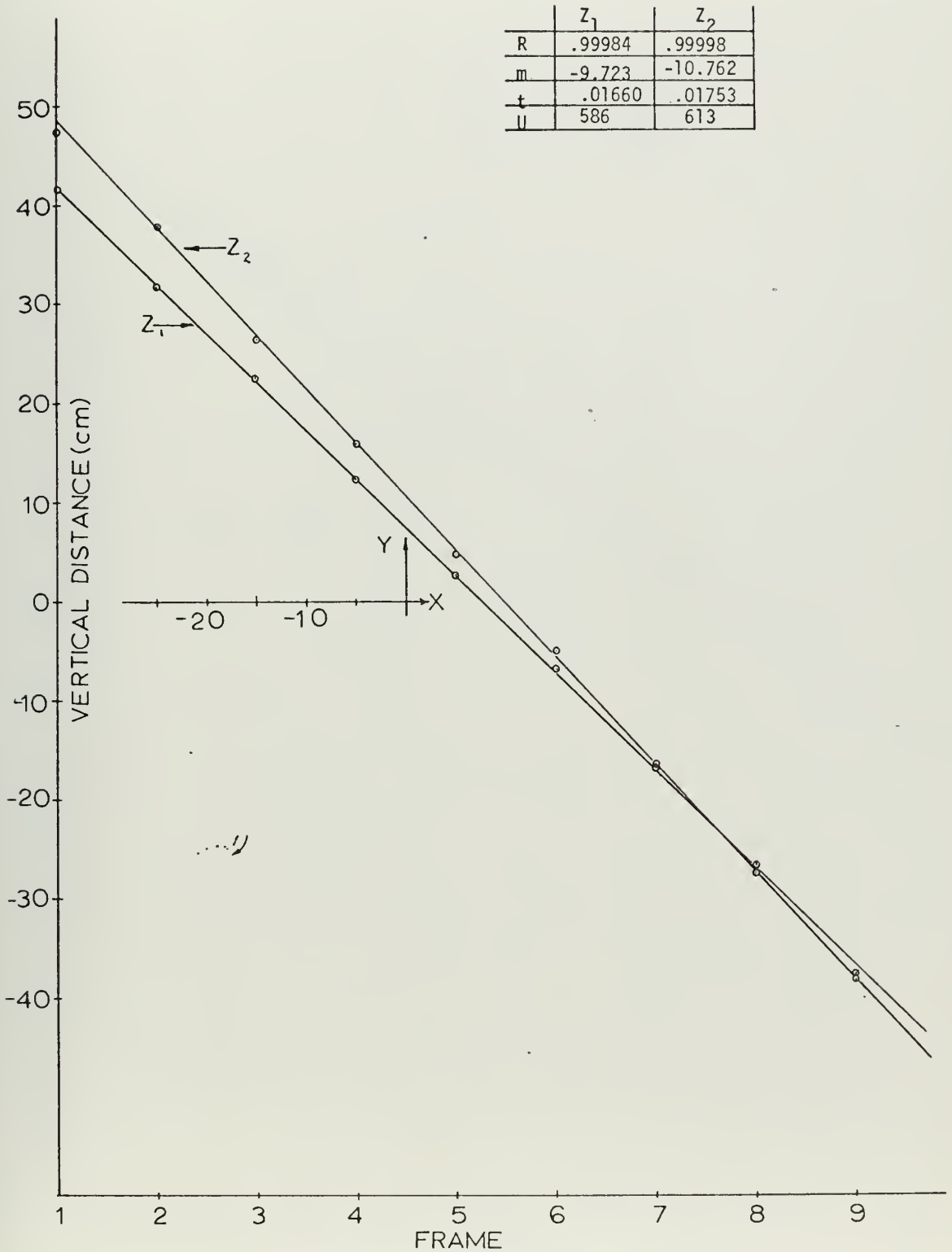

Figure 11. Data Run #3 Sphere #3

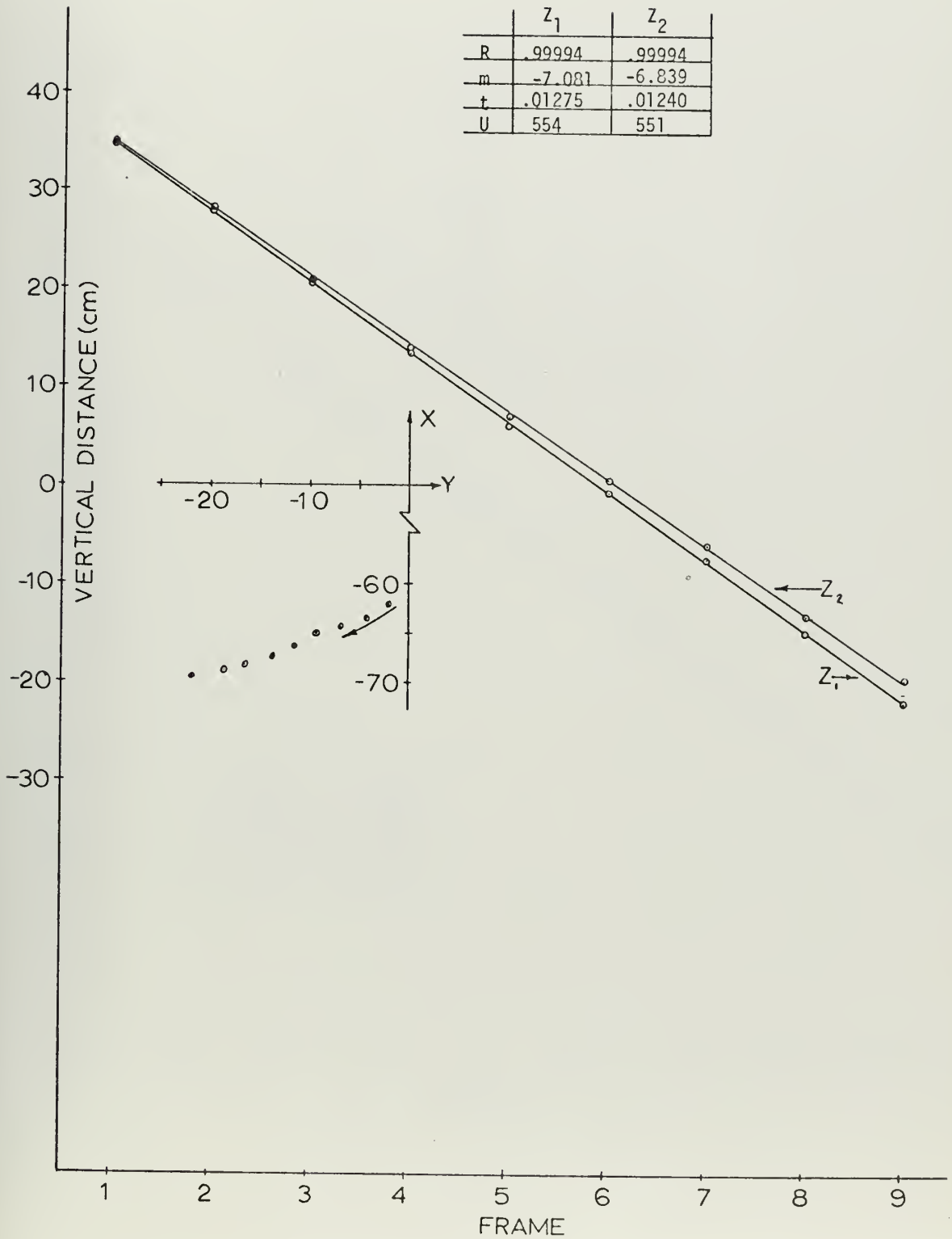

Figure 12. Data Run #5 Sphere #3

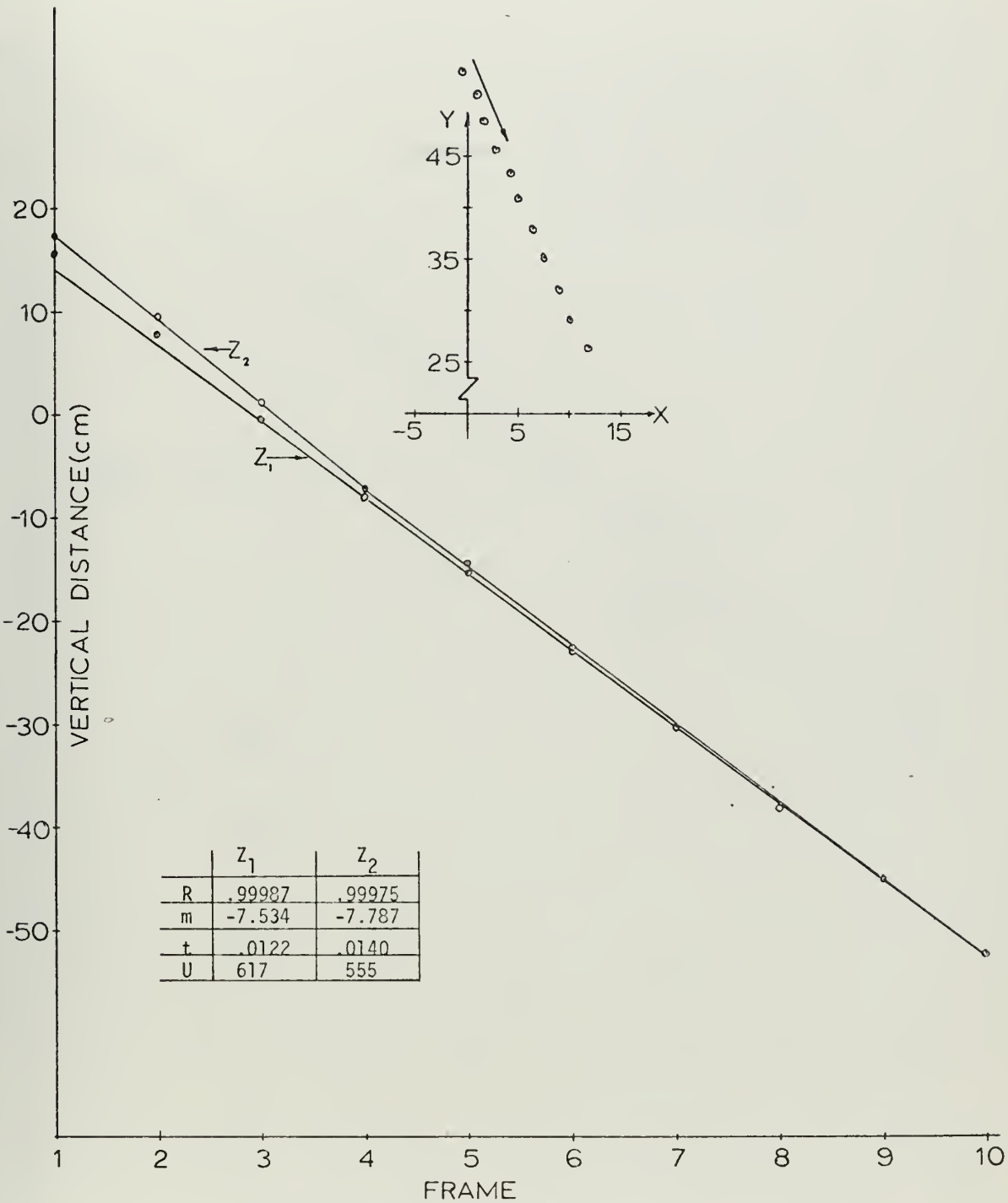

	Z_1	Z_2
R	.99987	.99975
m	-7.534	-7.787
t	.0122	.0140
U	617	555

Figure 13. Data Run #3 Sphere #4

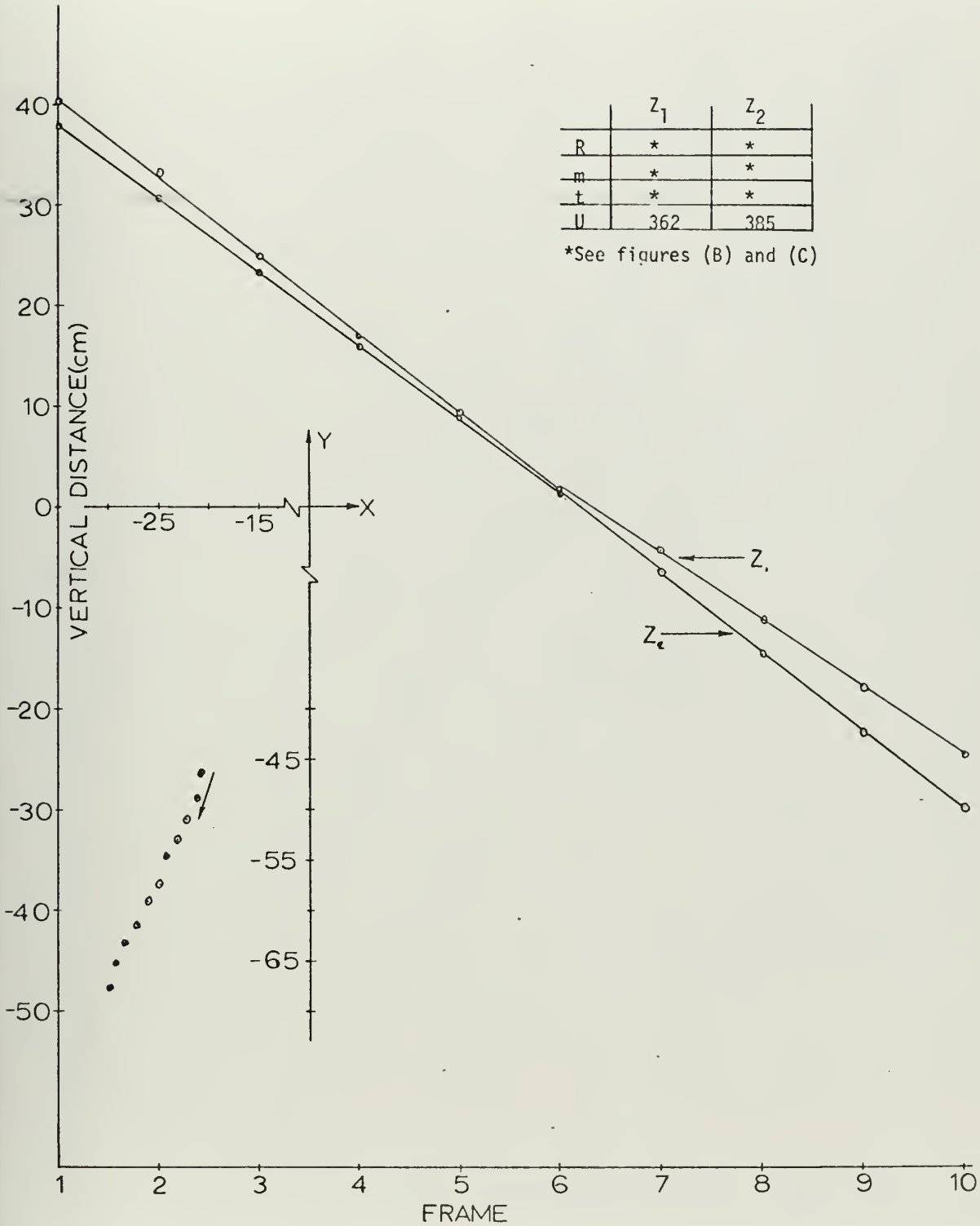

	Z_1	Z_2
R	*	*
m	*	*
t	*	*
U	362	385

*See figures (B) and (C)

Figure 14. Data Run #1 Sphere #5

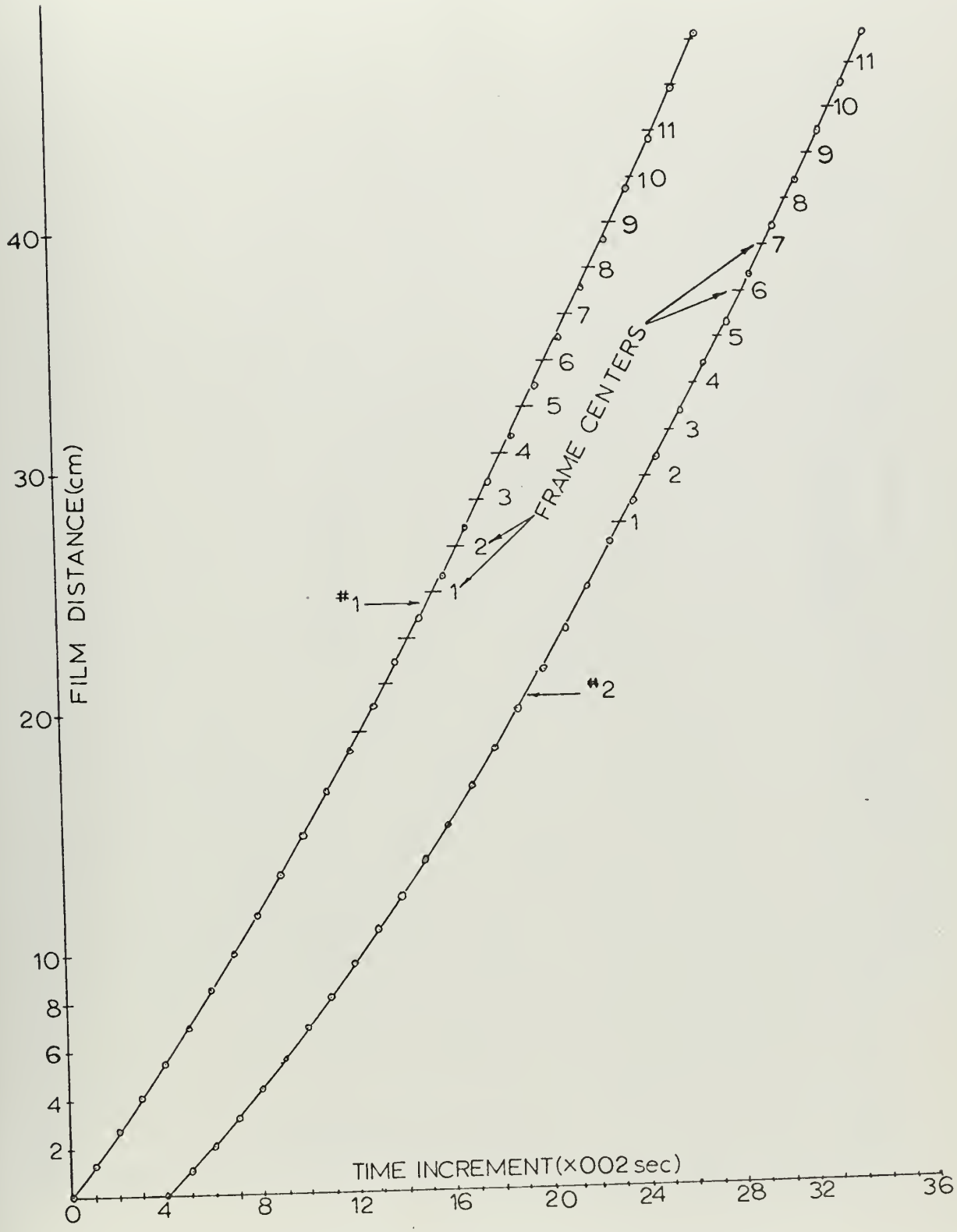

Figure 15. Film distance versus time marking Run #1 Sphere #5

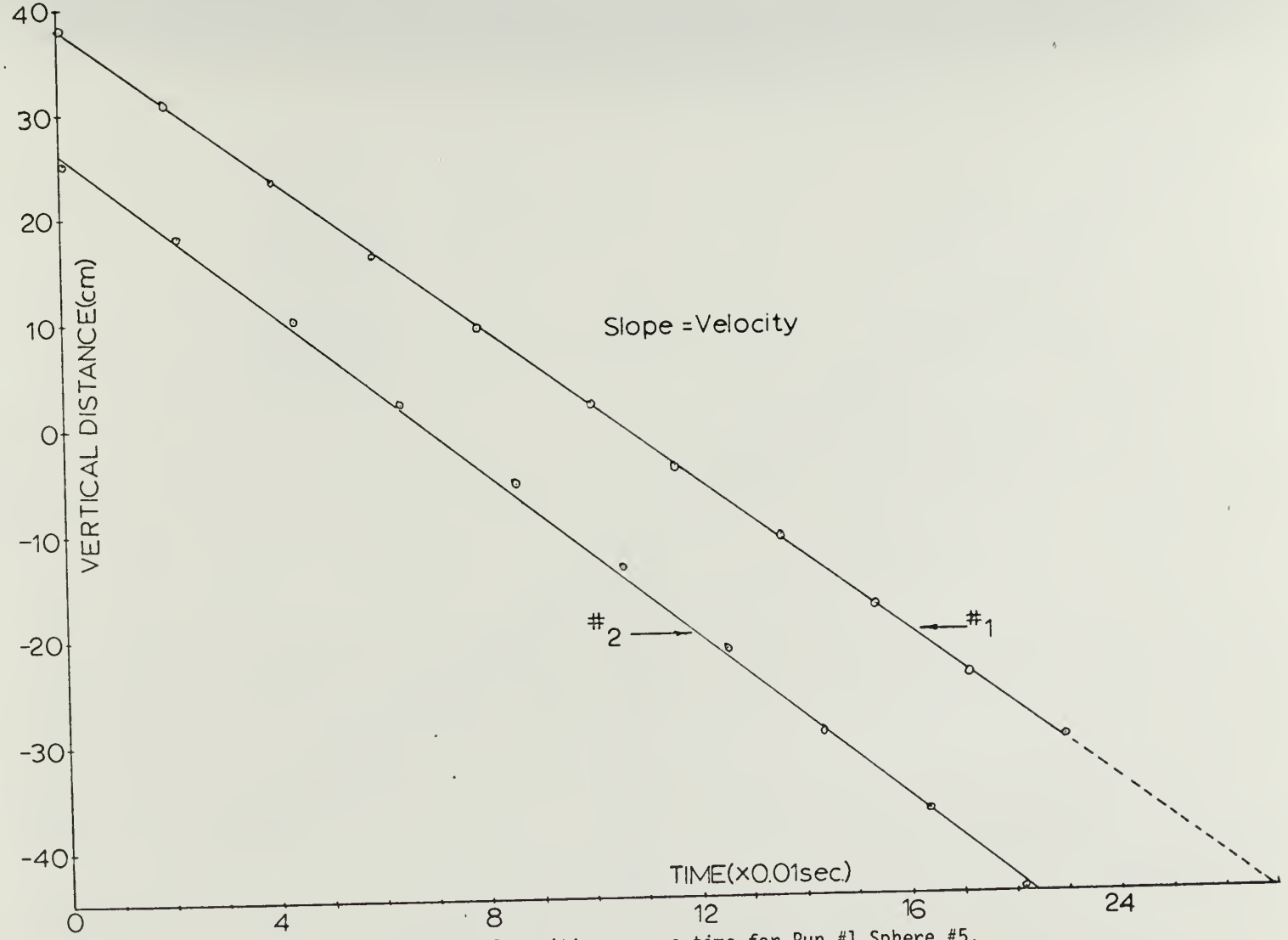

Figure 16. Vertical position versus time for Run #1 Sphere #5.

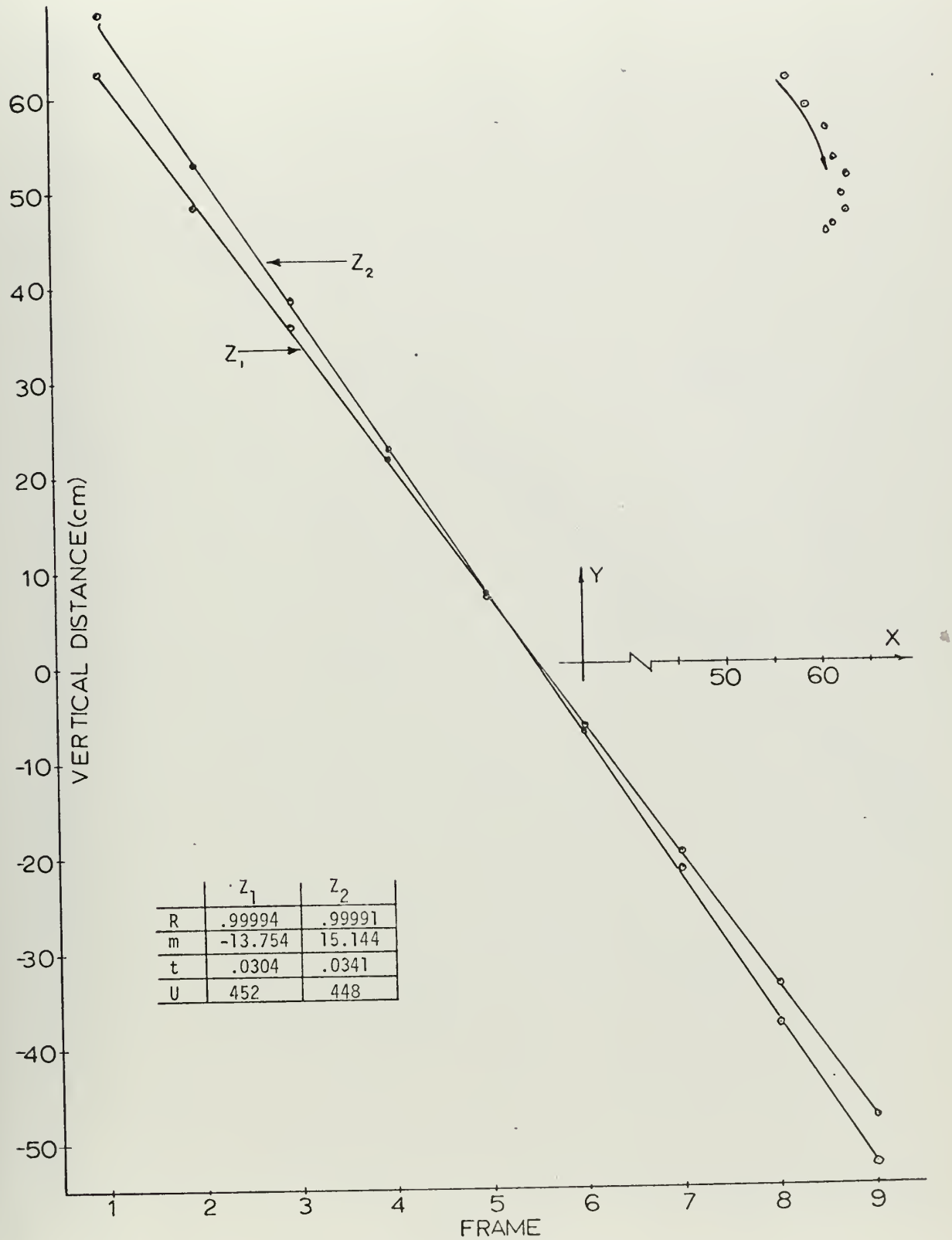

	Z_1	Z_2
R	.99994	.99991
m	-13.754	15.144
t	.0304	.0341
U	452	448

Figure 17. Data Run #2 Sphere #5.

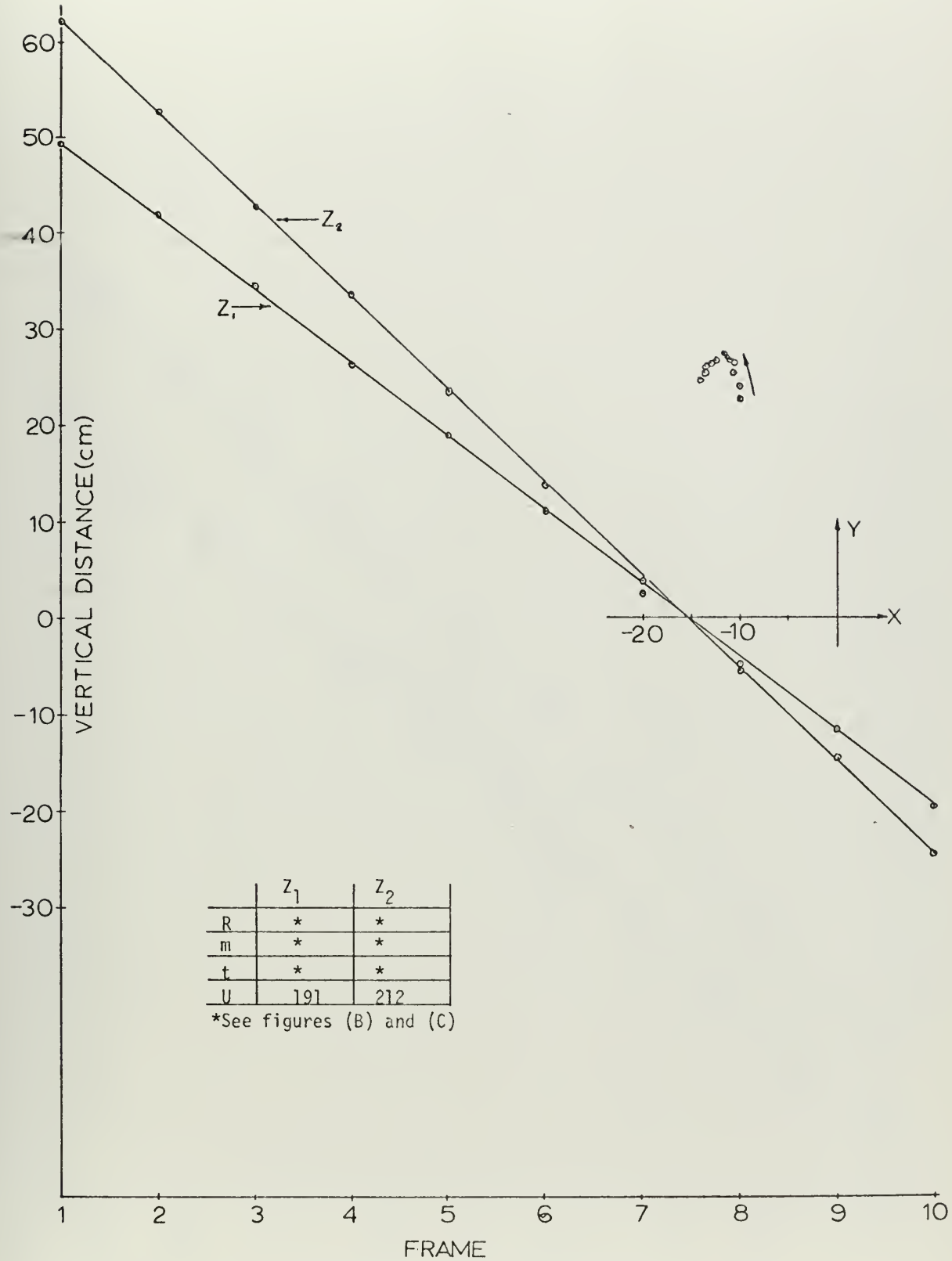

	Z_1	Z_2
R	*	*
m	*	*
t	*	*
U	191	212

*See figures (B) and (C)

Figure 18. Data Run #2 Sphere #6.

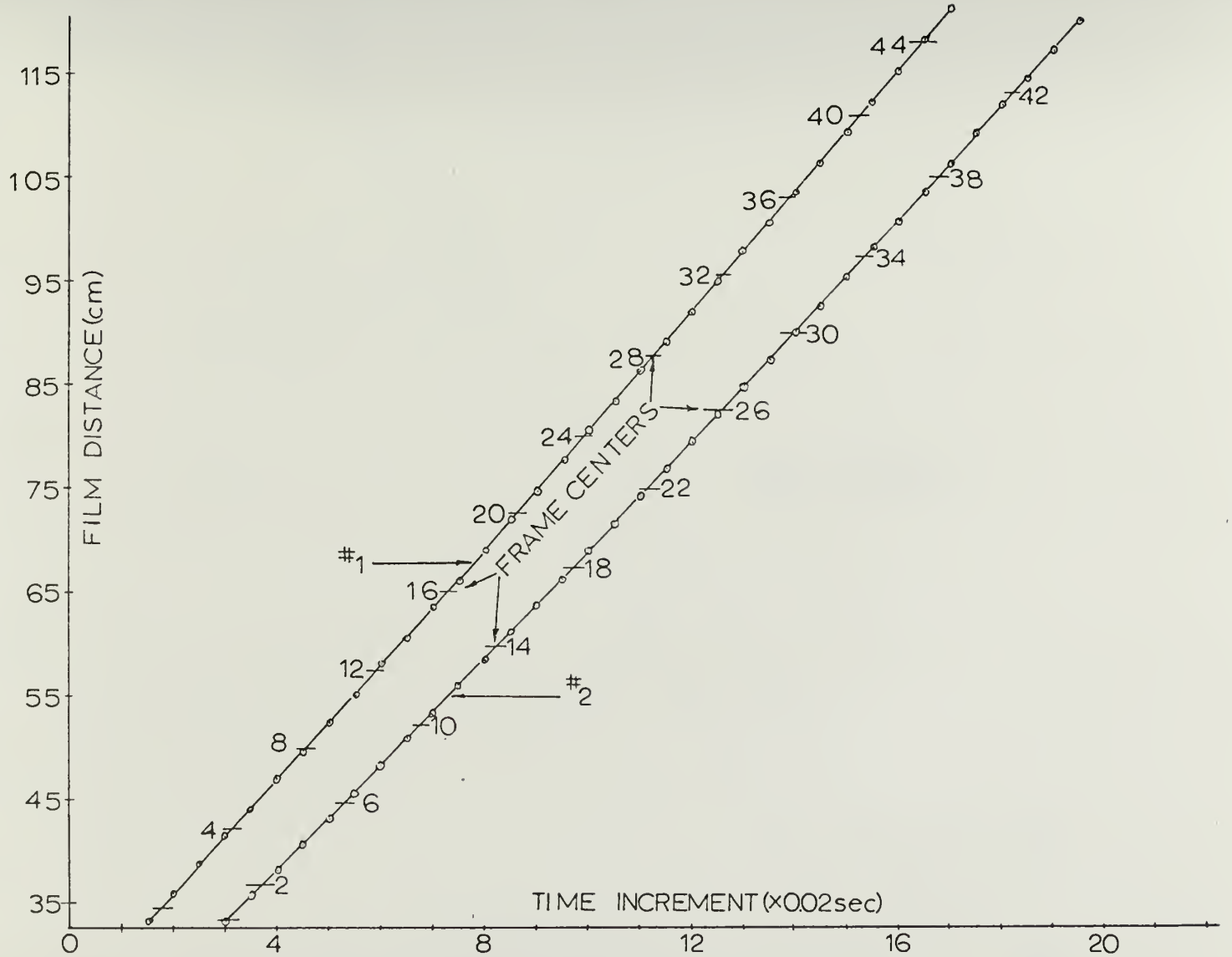

Figure 19. Film distance versus time marking Run #2 Sphere #6.

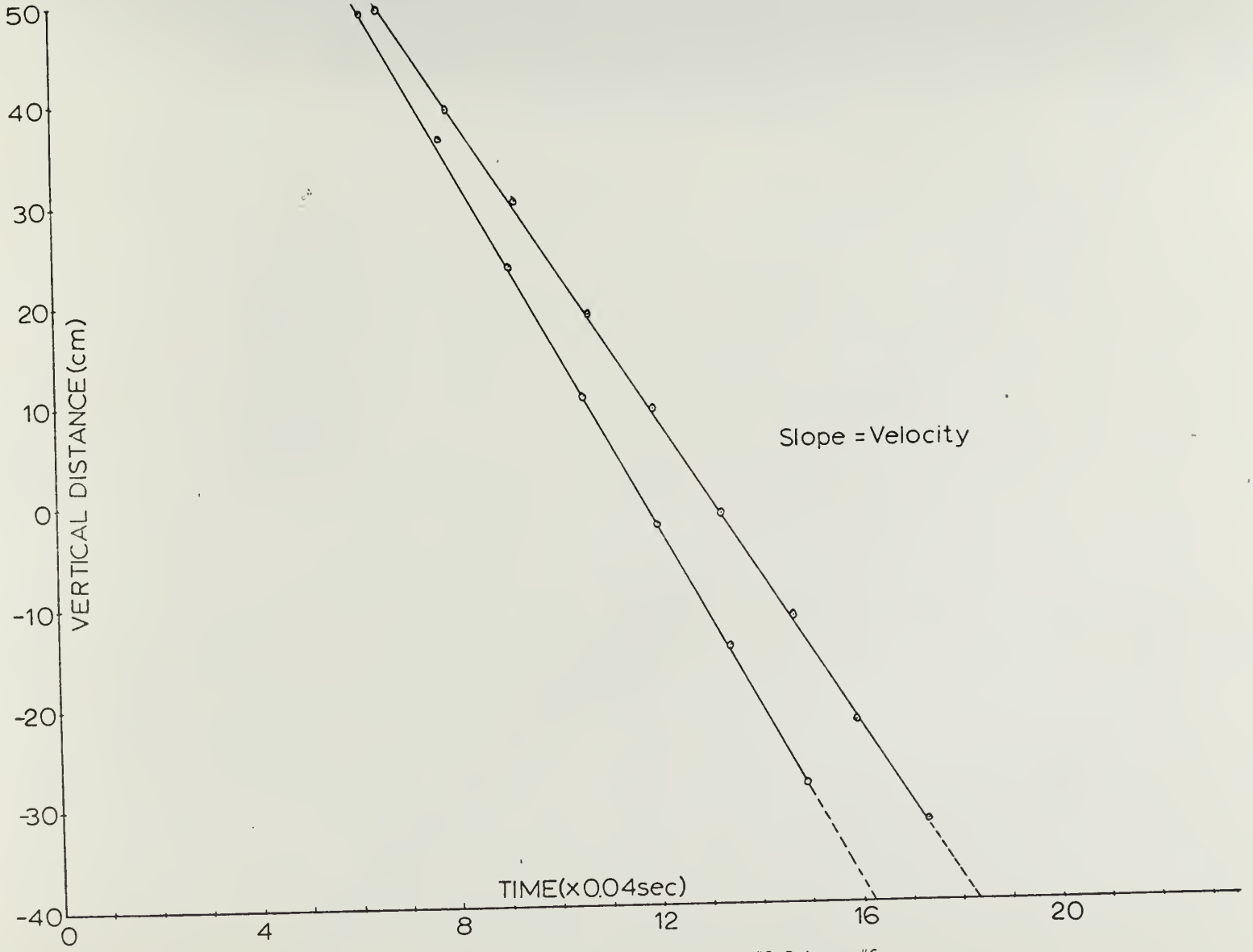

Figure 20. Vertical position versus time Run #2 Sphere #6.

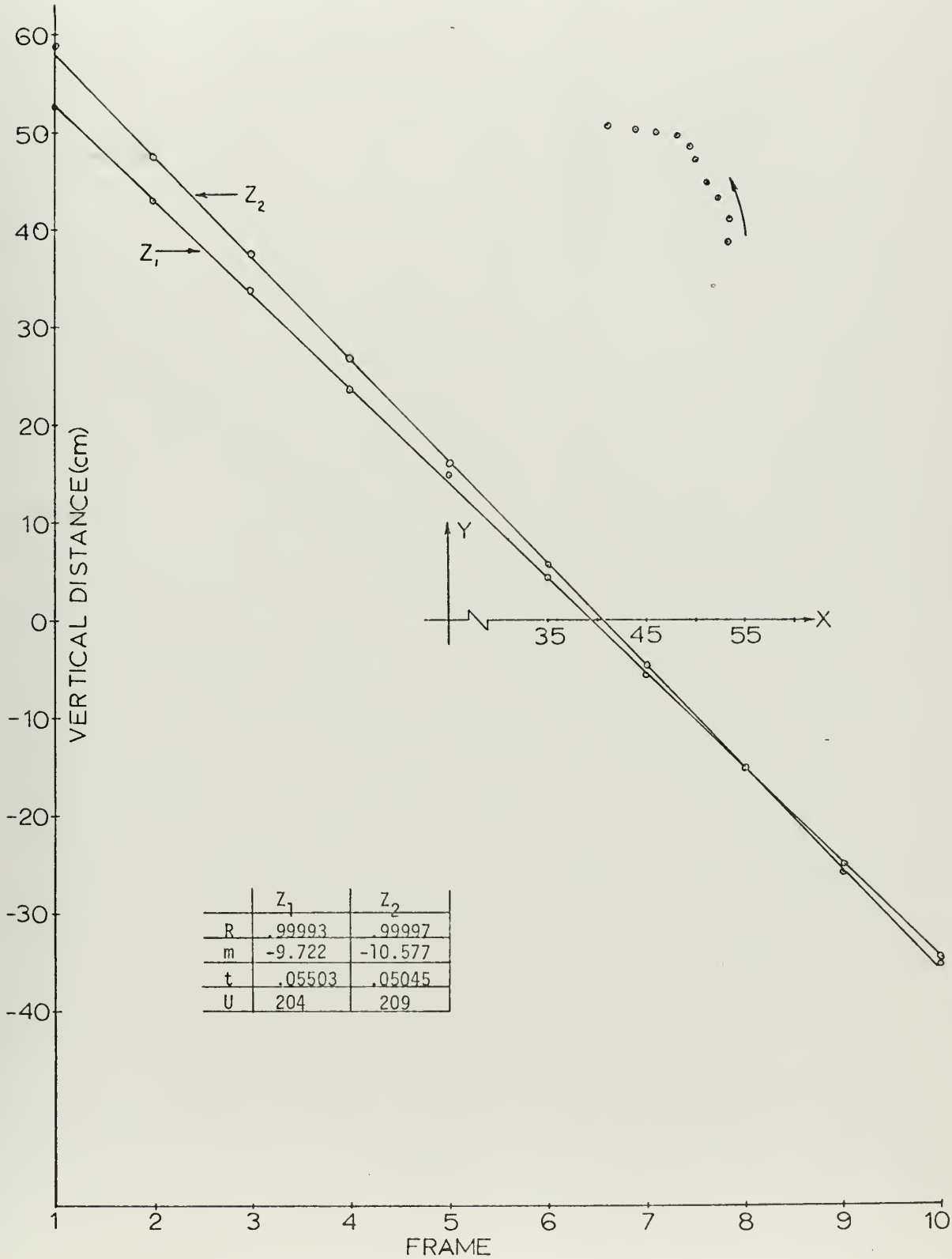

	Z_1	Z_2
R	.99993	.99997
m	-9.722	-10.577
t	.05503	.05045
U	204	209

Figure 21. Data Run #3 Sphere #6

	Z_1	Z_2
R	.99995	.99995
m	-7.260	-7.560
t	.03558	.03582
U	204	211

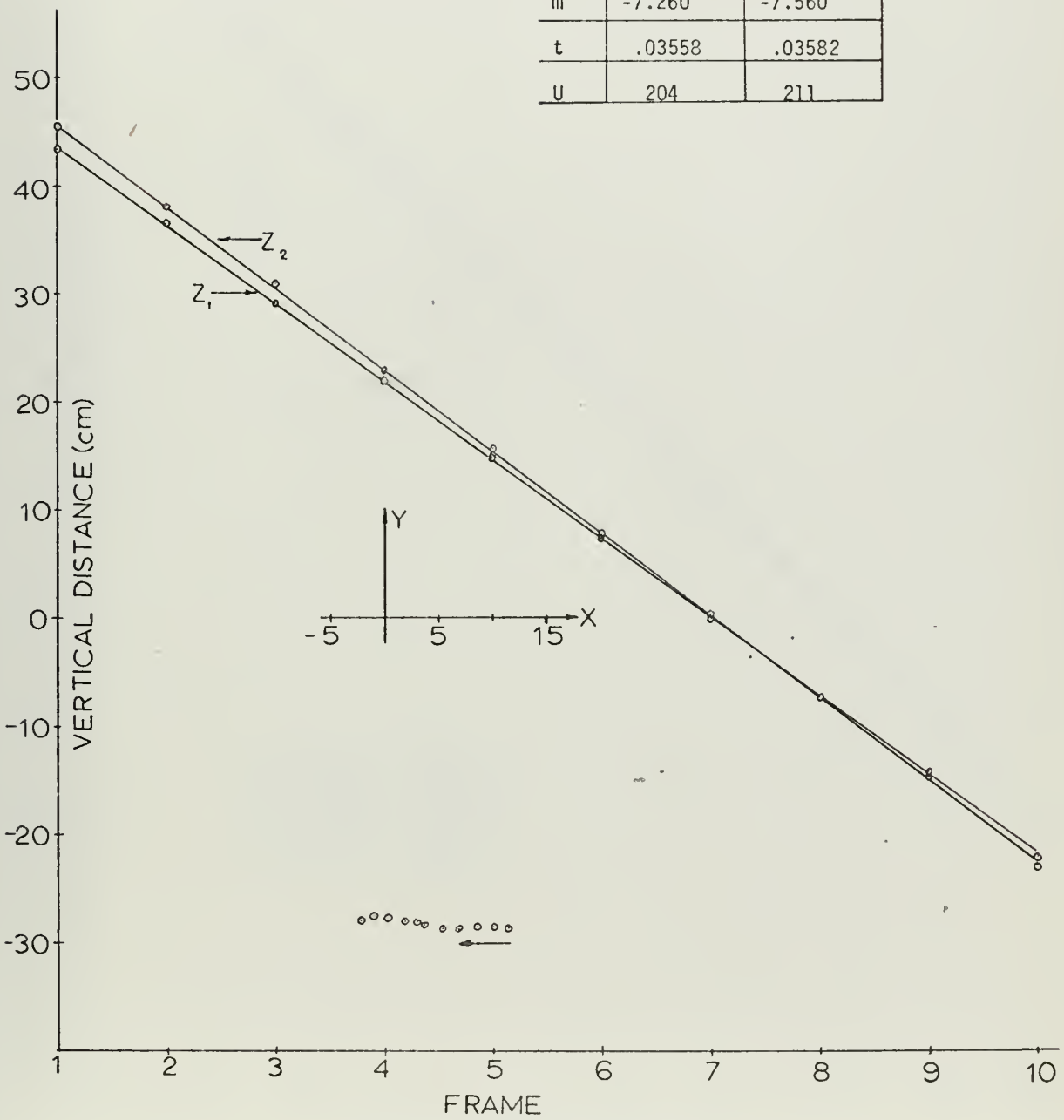

Figure 22. Data Run #5 Sphere #6.

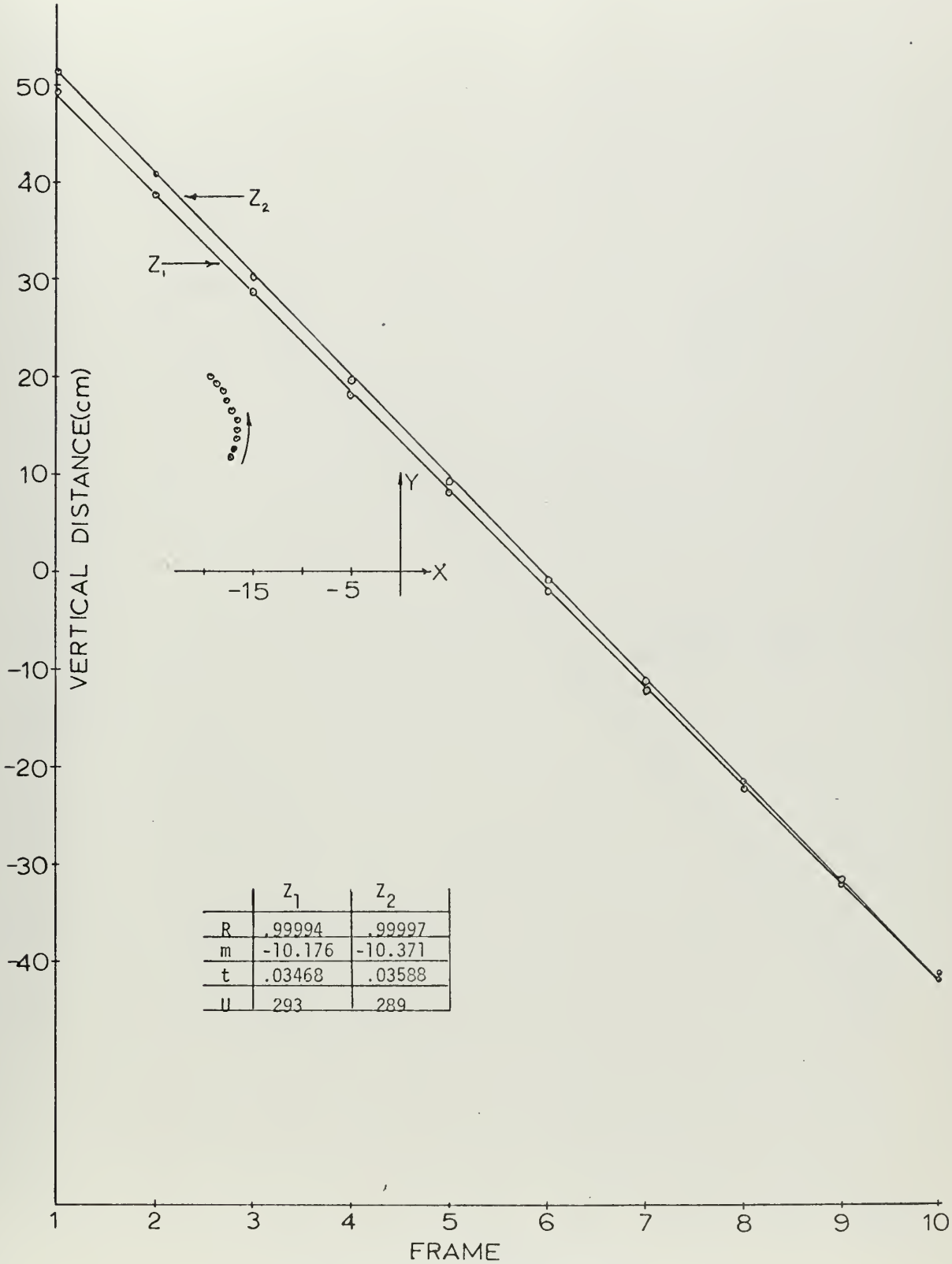

	Z_1	Z_2
R	.99994	.99997
m	-10.176	-10.371
t	.03468	.03588
U	293	289

Figure 23. Data Run #1 Sphere #7

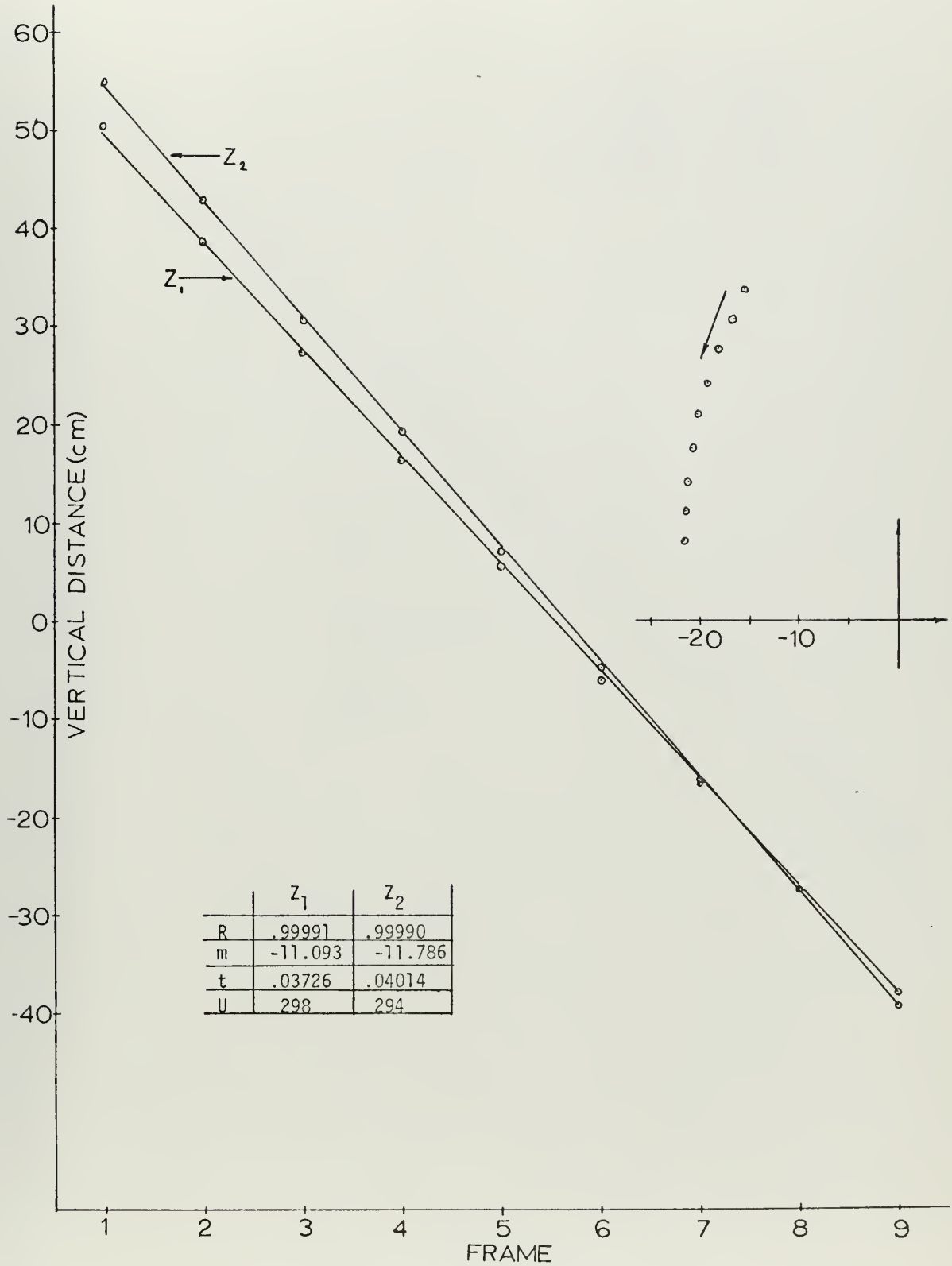

	Z_1	Z_2
R	.99991	.99990
m	-11.093	-11.786
t	.03726	.04014
U	298	294

Figure 24. Data Run #3 Sphere #7.

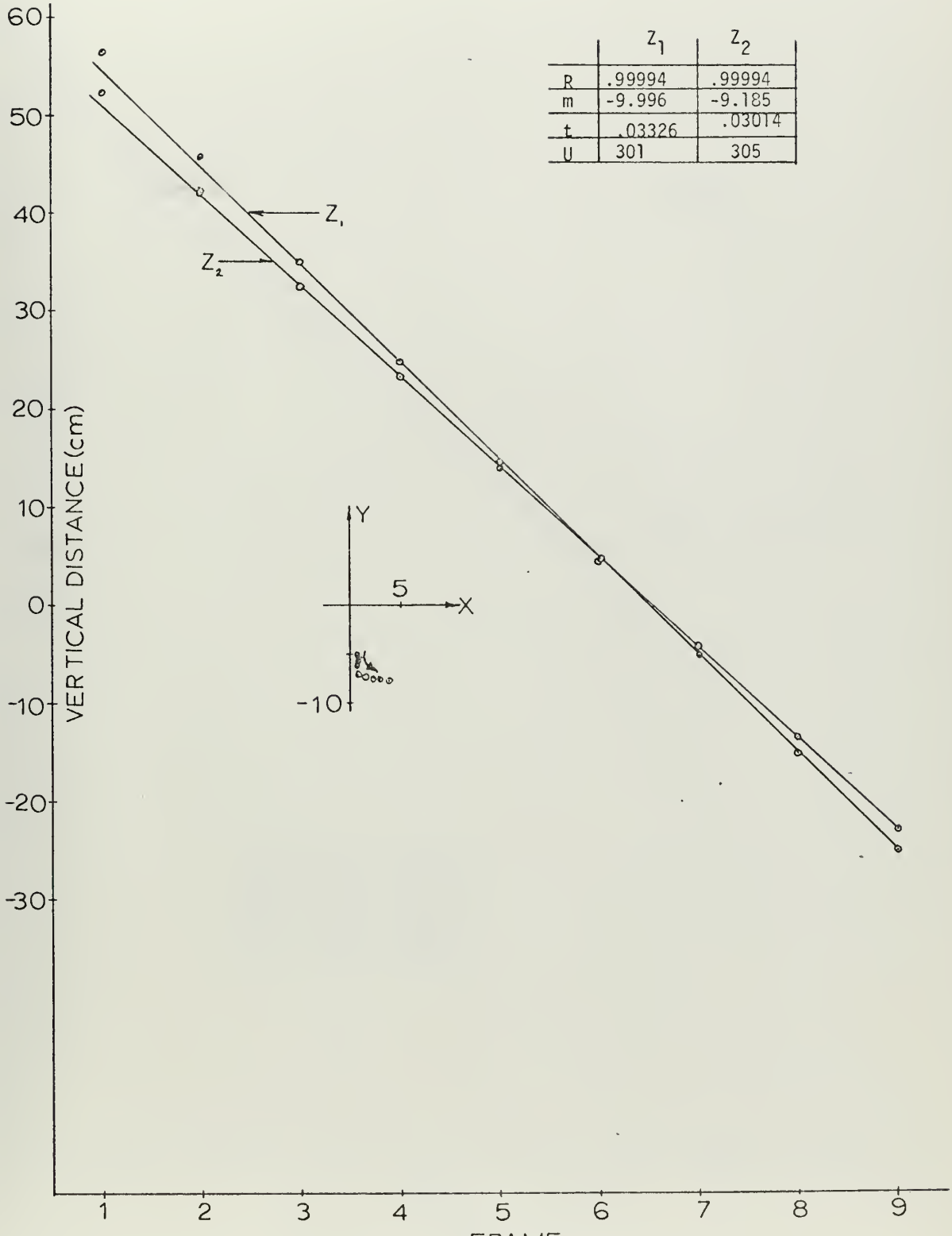

	Z_1	Z_2
R	.99994	.99994
m	-9.996	-9.185
t	.03326	.03014
U	301	305

Figure 25. Data Run #5 Sphere #7

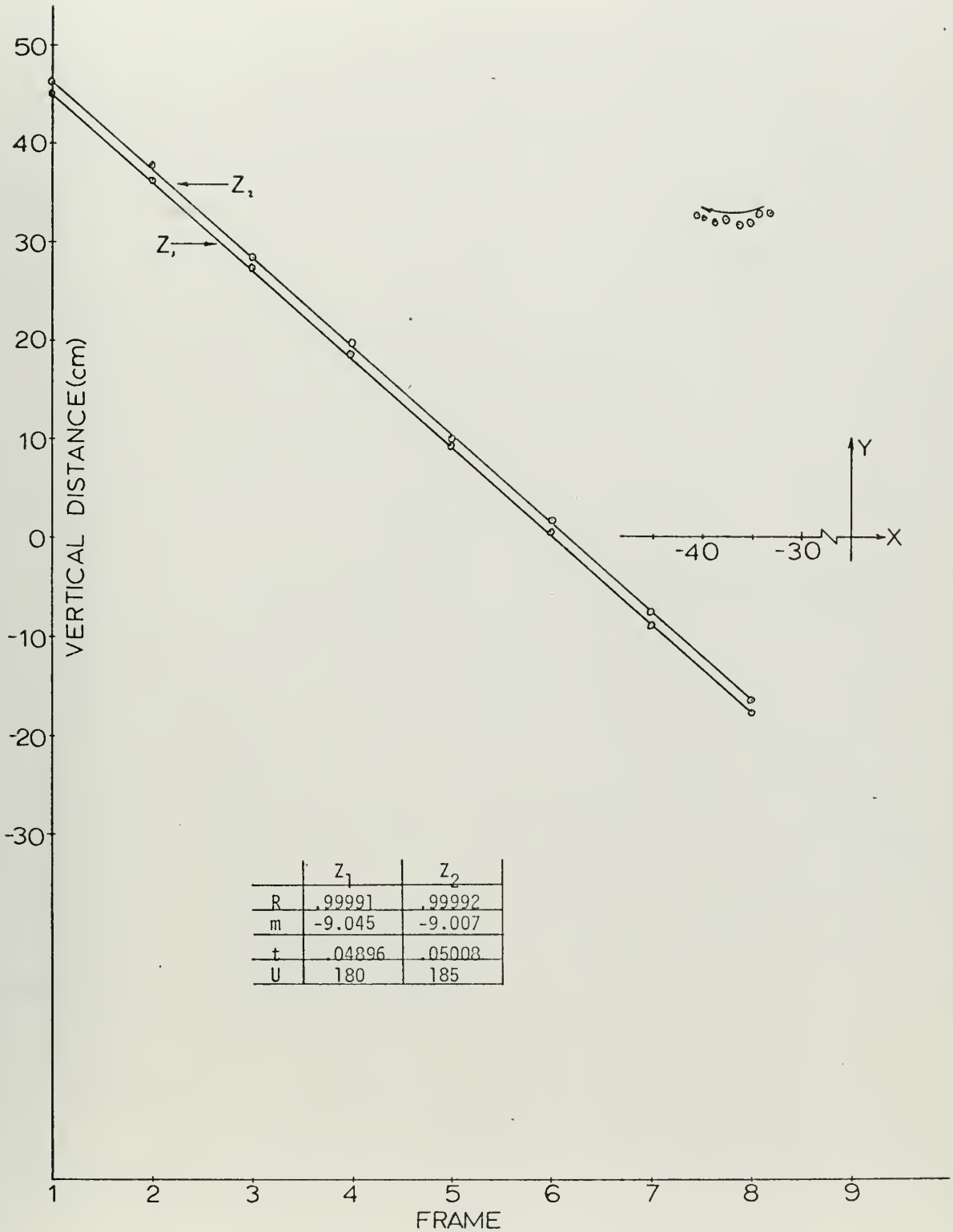

	Z_1	Z_2
R	.99991	.99992
m	-9.045	-9.007
t	.04896	.05008
U	180	185

Figure 26. Data Run #1 Sphere #8

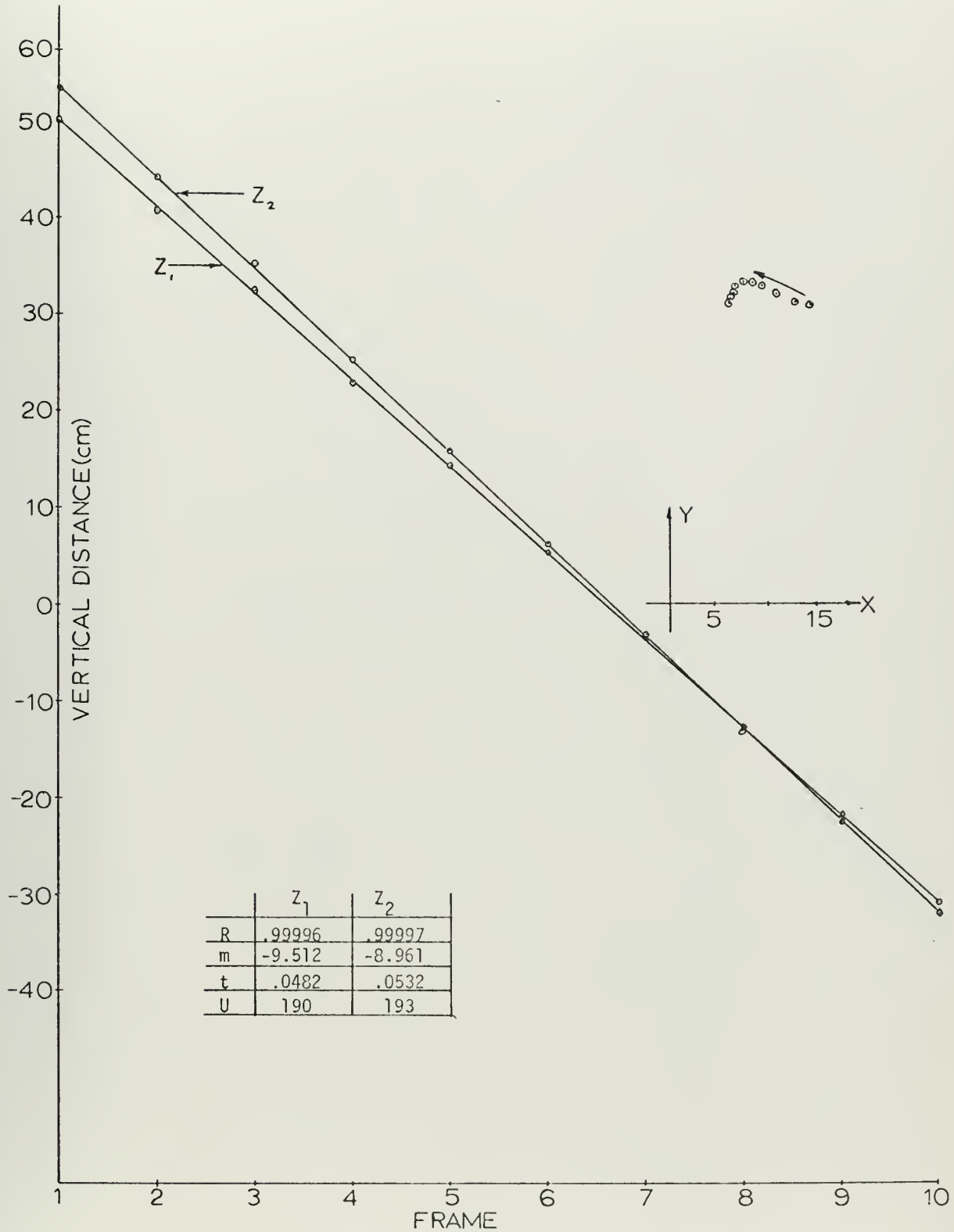

	Z_1	Z_2
R	.99996	.99997
m	-9.512	-8.961
t	.0482	.0532
U	190	193

Figure 27. Data Run #3 Sphere #8

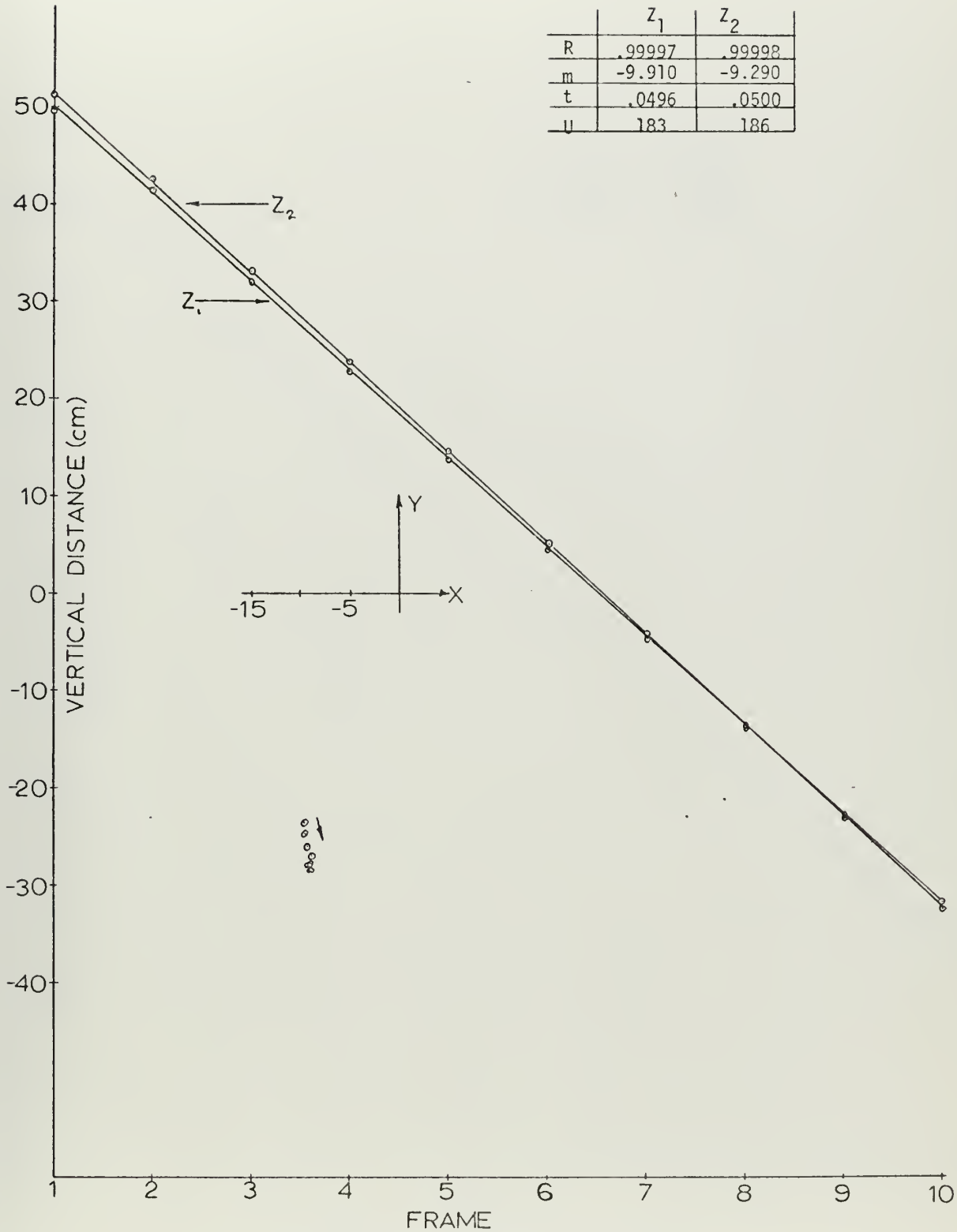

Figure 28. Data Run #4 Sphere #8

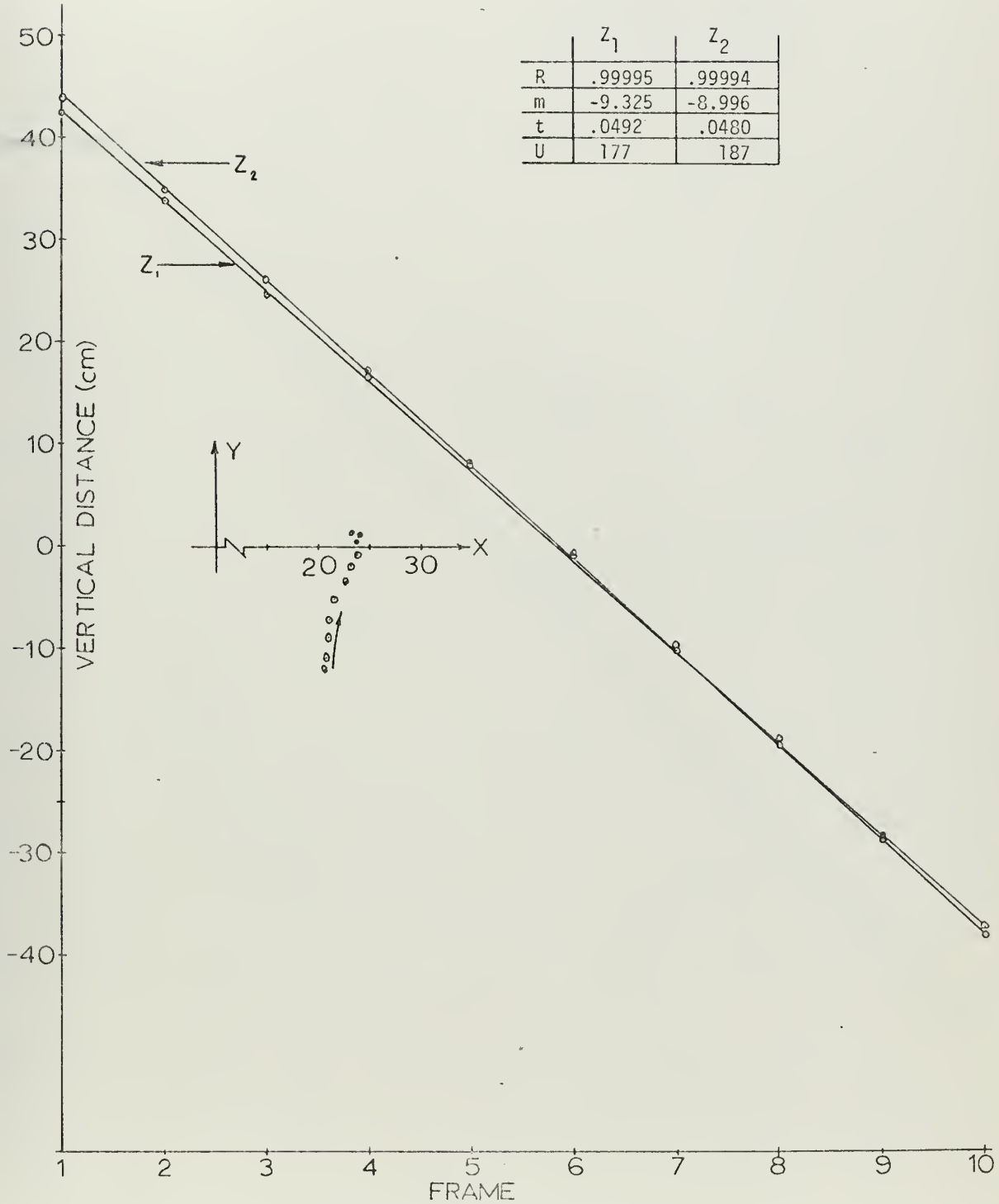

	Z_1	Z_2
R	.99995	.99994
m	-9.325	-8.996
t	.0492	.0480
U	177	187

Figure 29. Data Run #5 Sphere #8

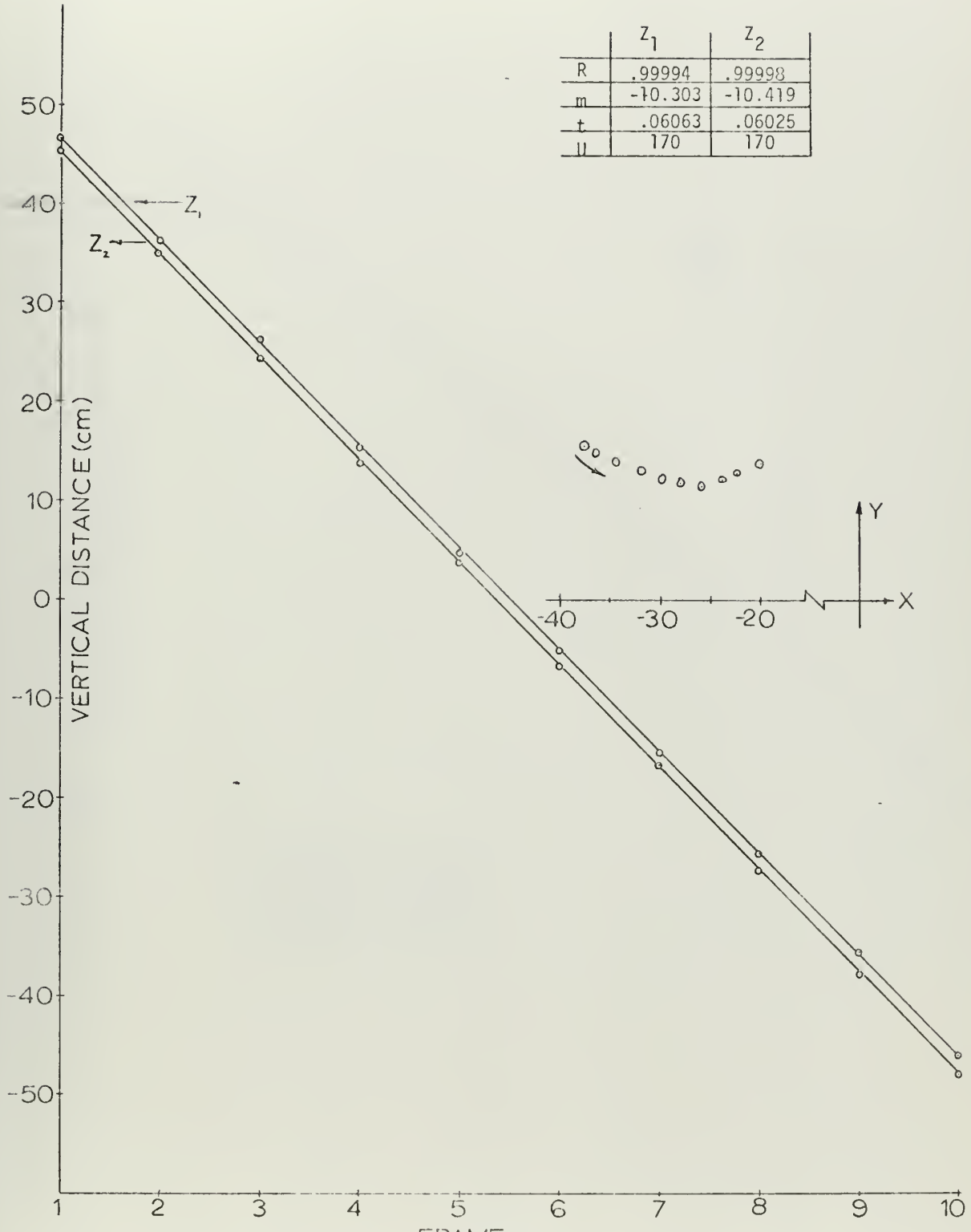

Figure 30. Data Run #1 Sphere #9

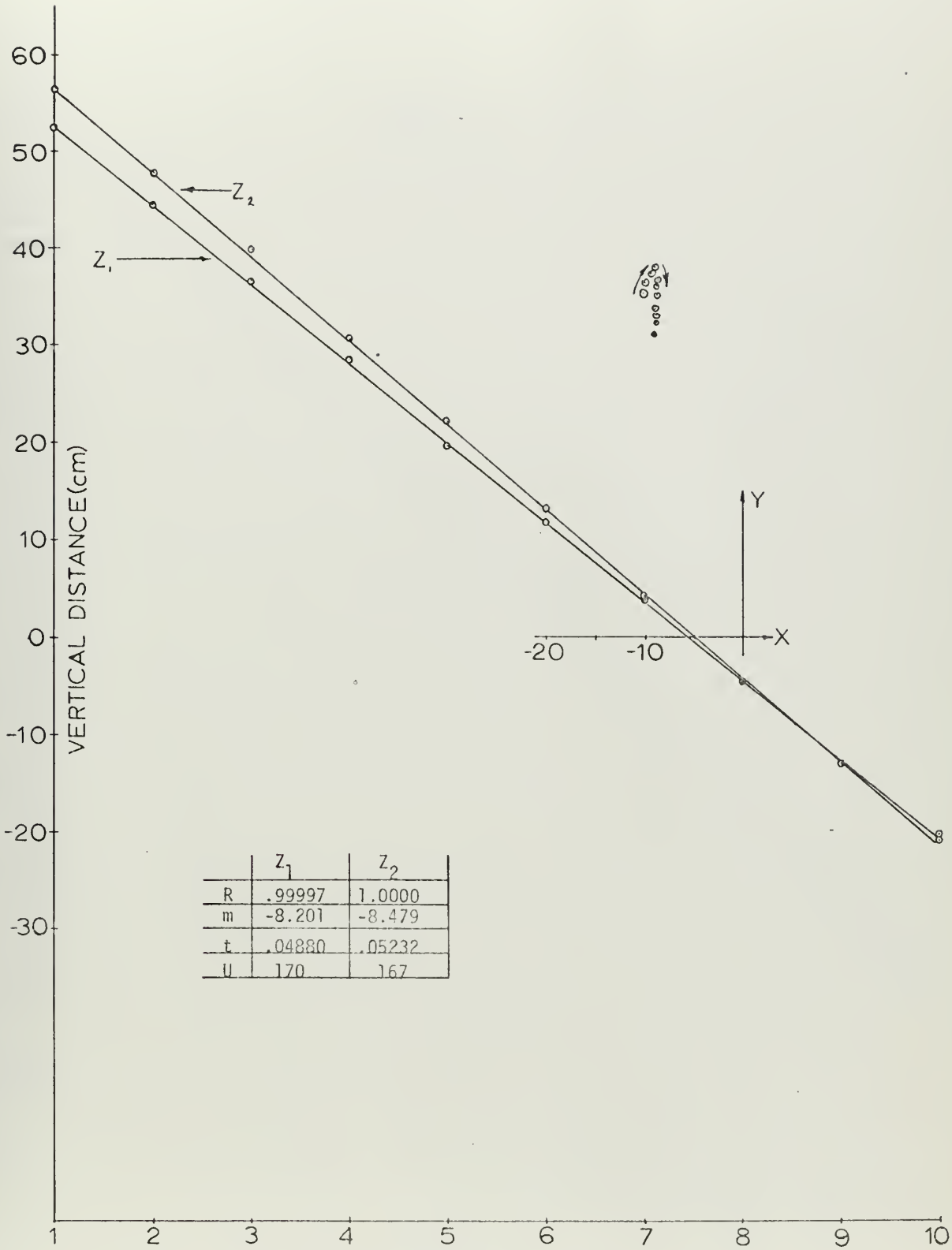

	Z_1	Z_2
R	.99997	1.0000
m	-8.201	-8.479
t	.04880	.05232
U	170	167

Figure 31. Data Run #2 Sphere #9

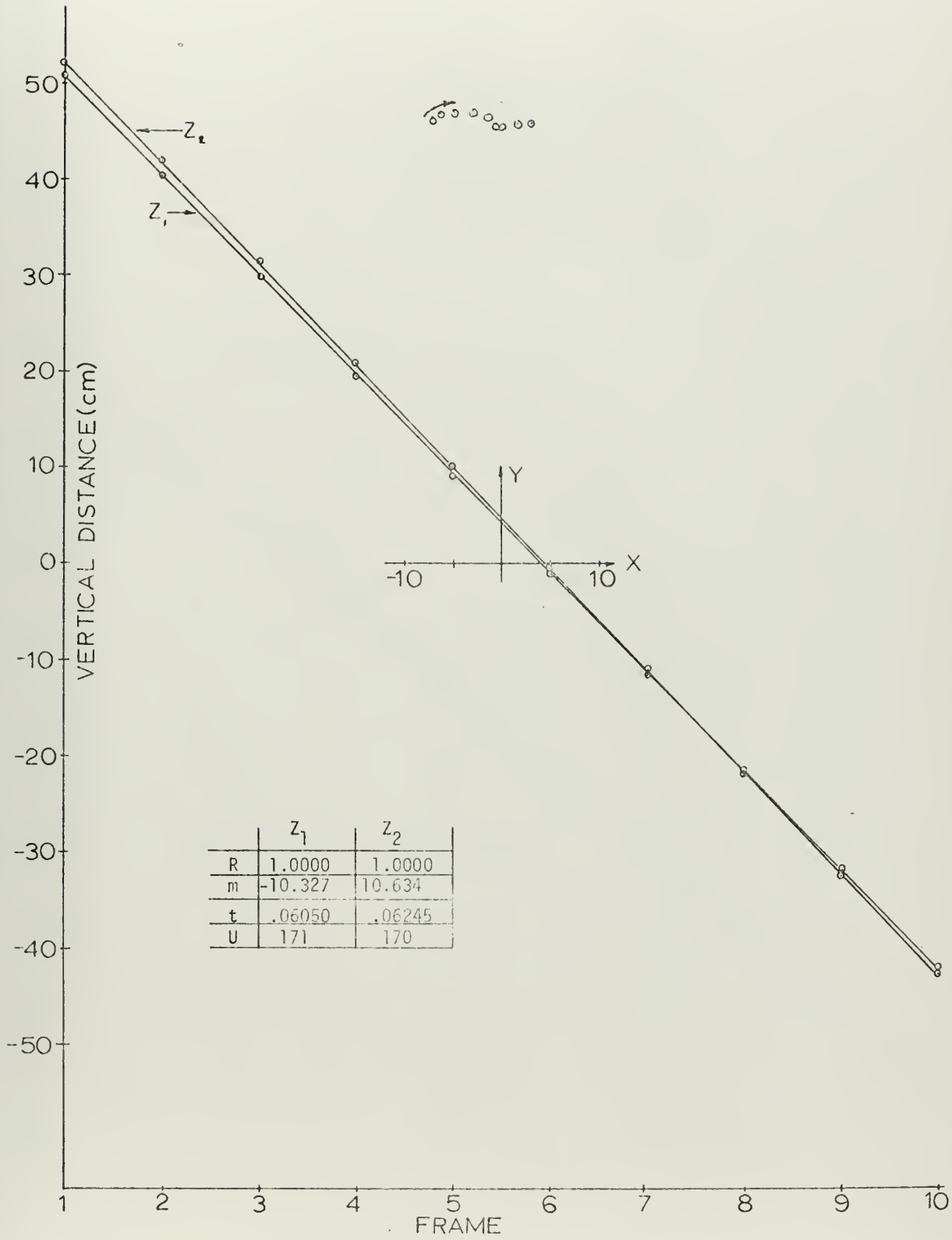

	Z_1	Z_2
R	1.0000	1.0000
m	-10.327	10.634
t	.06050	.06245
U	171	170

Figure 32. Data Run #3 Sphere #9.

	Z_1	Z_2
R	.99996	.99997
m	-7.860	-8.118
t	.0484	.0496
U	.162	.164

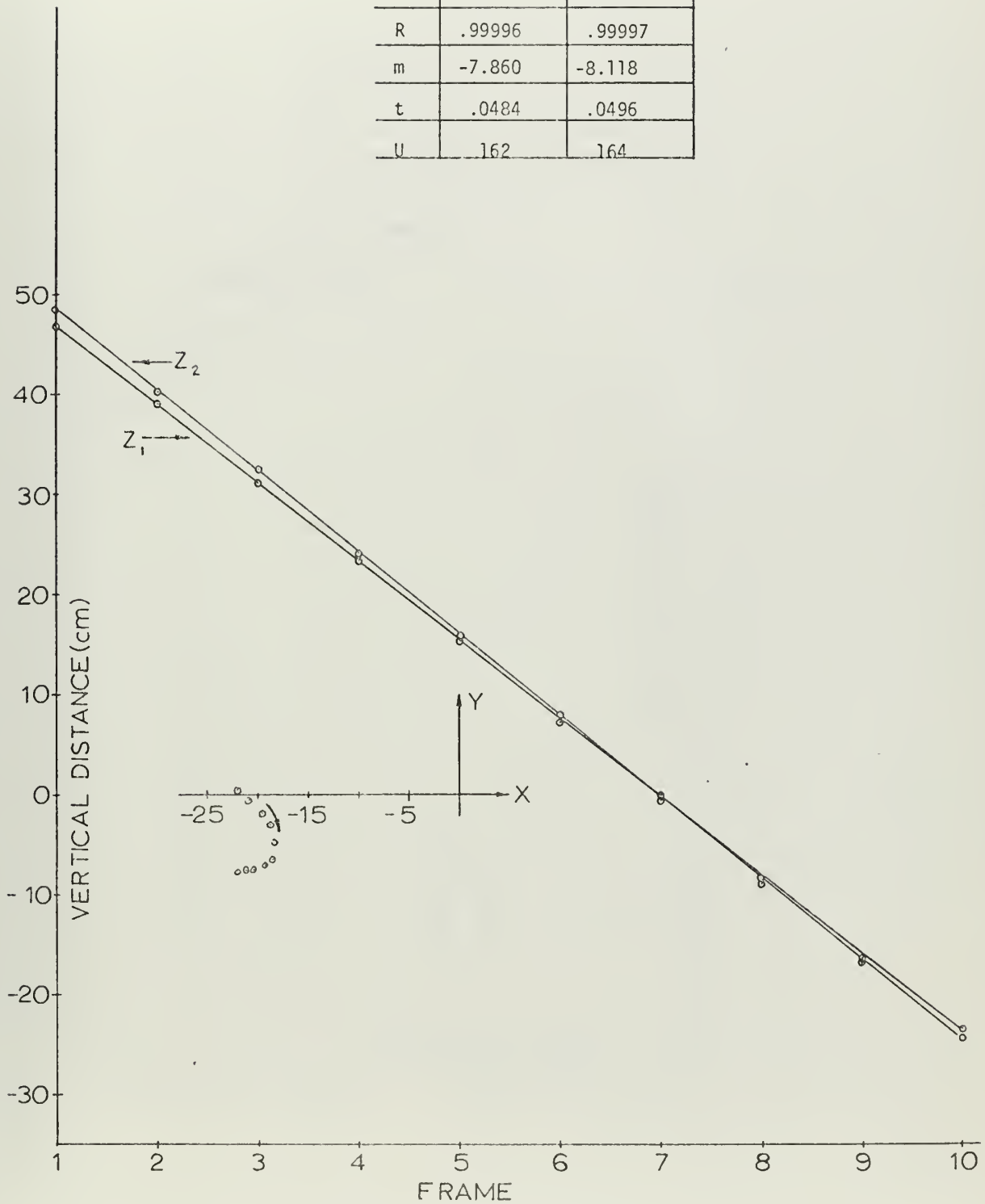

Figure 33. Run #4 Sphere #9.

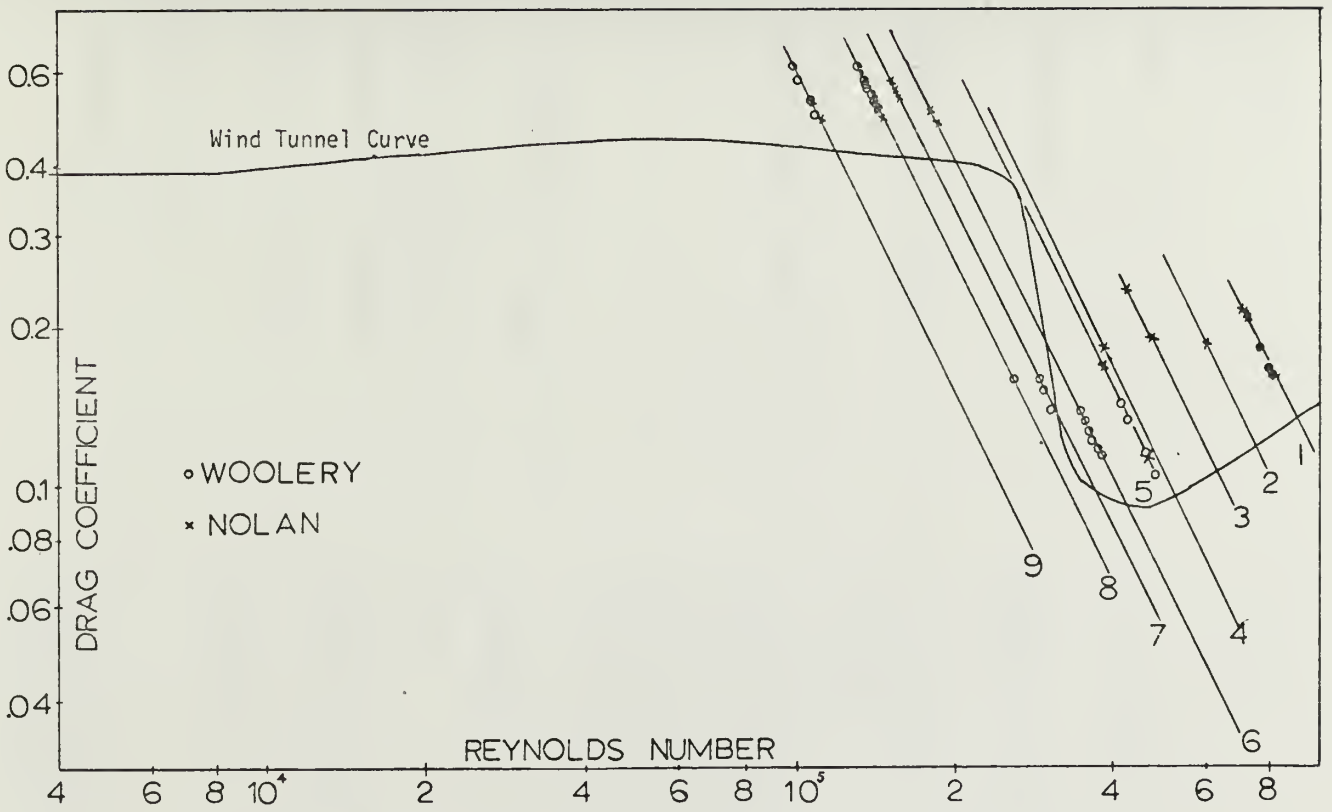

Figure 34. Measured Sphere Drag Coefficients in Water.

APPENDIX A

Summary of the Variable Atmosphere Tank Characteristics

Tank:

Diameter	12 feet
Height	39 feet
Design pressure	Zero vacuum to one atmosphere pressurization
Access door	Located near the top of the tank. A monorail with 1/2-ton hoist runs through access door opening.
Observation windows	Five windows, each 28 inches wide by 76 high, are located up on side of tank.
Camera and lighting ports	Three columns of ports with 15 ports per column. Ports are on foot in diameter. Two columns of ports are located 45° either side of observation windows and the third column is 180° from observation windows.
Maximum water height	24.5 feet above submerged supporting platform.
Color of Interior	White
Supporting platform	Raised and lowered by a telescoping hydraulic lift.
Reference Markings	Surveyed in scribe marks. See figure 37.

Photographic Cameras:

Photosonic 1B	16mm rotating prism-type camera, framing rates of 12 to 1,000 frames/second, exposure time of 1/40,000 of a second.
Mitchell GC	35mm dual pin register, intermittant movement, maximum framing rate of 128 frames per second., shutter adjustment of 0°- to 170°.

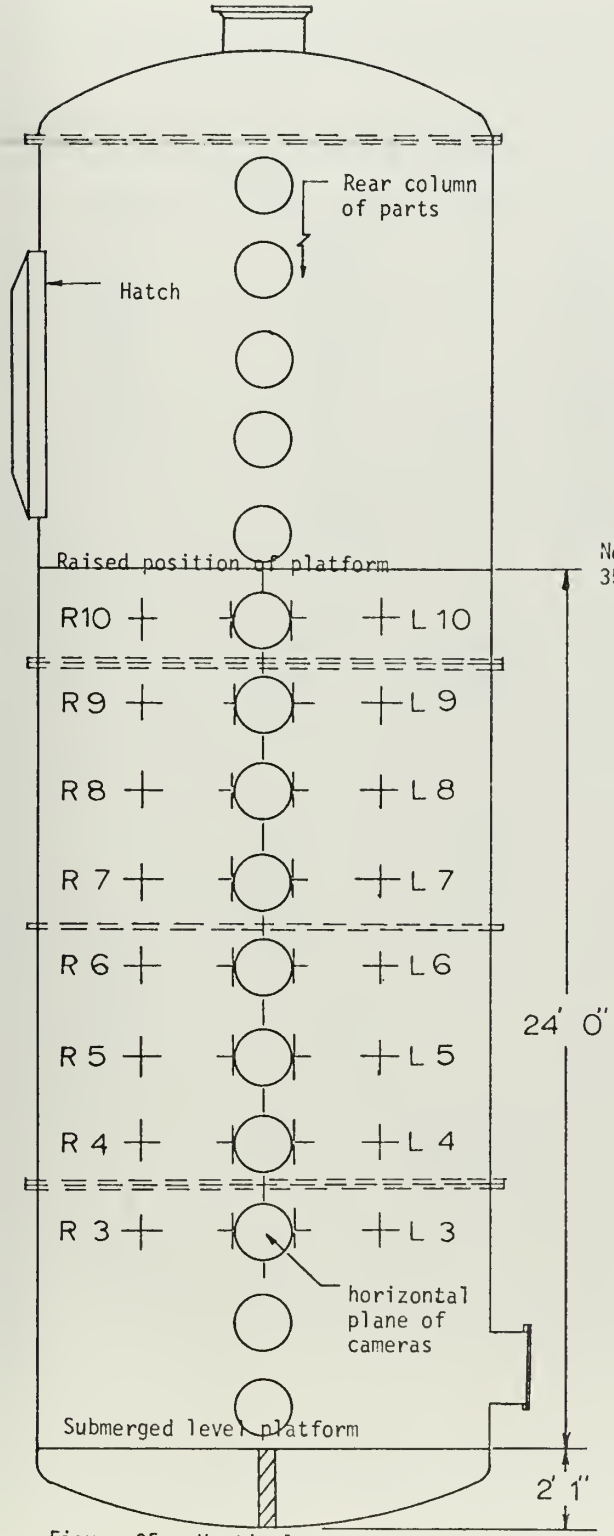

Figure 35. Vertical cross section of VAT.

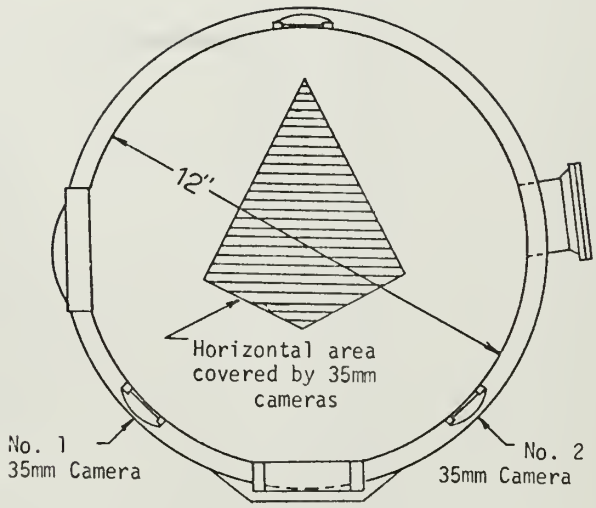

Figure 36. Horizontal cross section of VAT.

Distance from Lens	Height	Width
6'	3' 7"	5' 3"
7'	4' 5"	6' 2"

TABLE II. 35mm camera vertical plane coverage data.

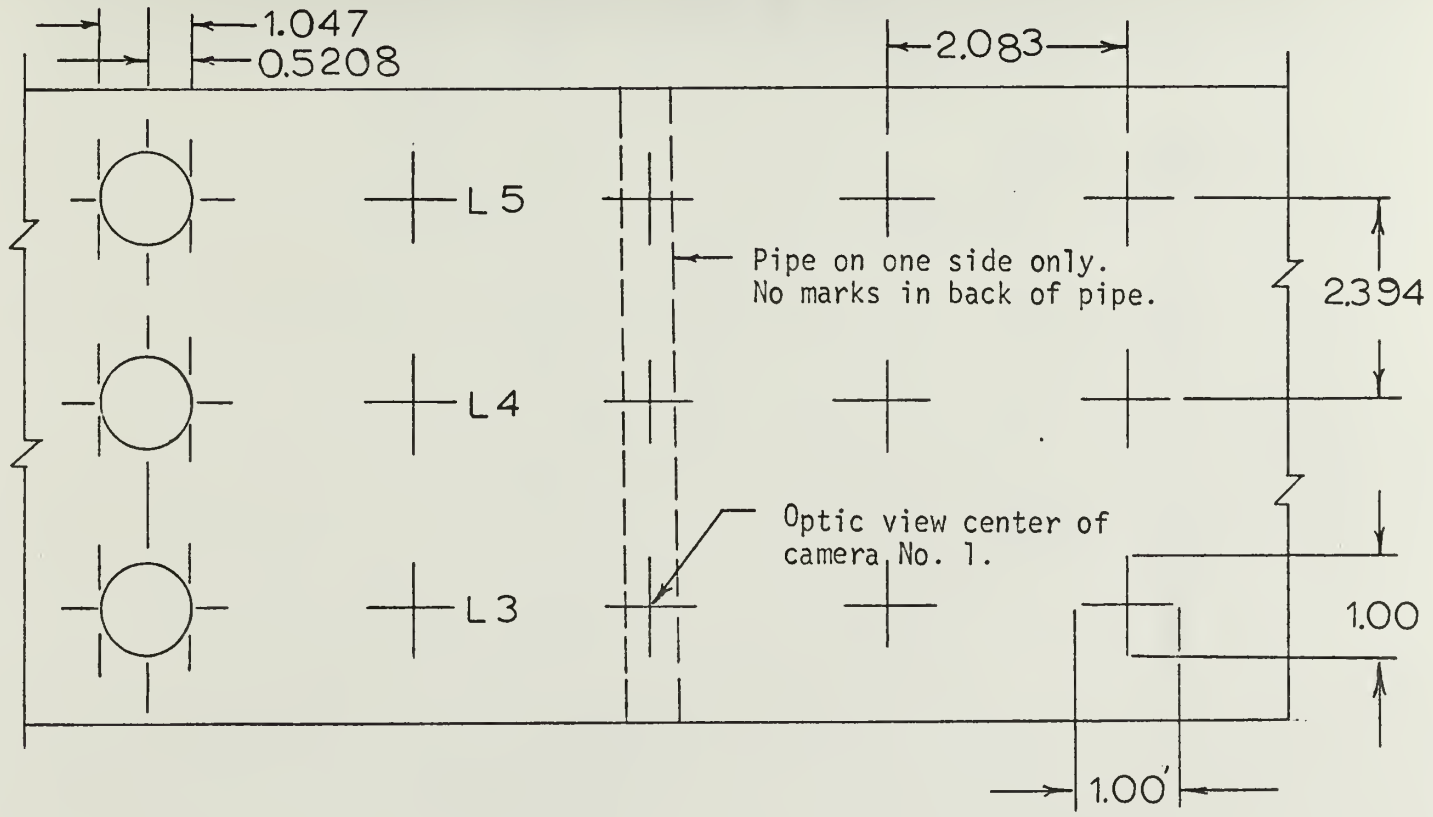

Figure 37. Blow up of the left side of the VAT showing the optical center of No. 1 camera. Parts shown are the rear parts.

APPENDIX B

Program A

From figures 4 and 5

$$R_1 = L_1 \tan \theta_1 + (b + X_1) \tan \theta_1'$$

$$R_2 = L_2 \tan \theta_2 + (b + Y_2) \tan \theta_2'$$

$$R_1 = \frac{Z_1}{\cos \phi_1} \quad \text{where } \cos \phi_1 = \frac{z_1}{r_1}$$

$$R_2 = \frac{Z_2}{\cos \phi_2} \quad \text{where } \cos \phi_2 = \frac{z_2}{r_2}$$

$$\sin \theta' = \frac{\sin \theta}{n}$$

Known: L_2, L_1, I, b

Measured: x_2, y_1, z_1, z_2

Assume: $x_1 = x_2$ and $y_1 = y_2$

$$Z_1 - \tan \phi_2 \tan \phi_1' \cos \phi_1 Z_2 = (L_1 \tan \theta_1 + b \tan \theta_1') \cos \phi_1$$

$$- (\tan \phi_1 \tan \theta_2' \cos \phi_2) Z_1 + Z_2 = (L_2 \tan \theta_2 + b \tan \theta_2') \cos \phi_2$$

$$X = Z_2 \tan \phi_2$$

$$Y = Z_1 \tan \phi_1$$

Step	Key	Code	x	y	z	f	e	d	c	b	a
0	0 Clear	20									
	1 Stop	41	y_1'	y_1'	z_1'						
	2 .	21									
	3 0	00									
	4 0	00									
	5 0	00									
	6 3	03									
	7 5	05									
	8 5	05	.000355	y_1'	z_1'						
	9 X	36		y_1'	z_1'						
	a Roll ↑	22	z_1'	.000355	y_1						
	b X	36	.	z_1	y_1						
	c ↓	25	z_1	y_1	y_1						
	d ↑	27	z_1	z_1	y_1						
	0 Roll ↓	31	z_1	y_1	z_1						
	1 Polar	62	$\lvert r_1 \rvert$	ϕ_1							
	2 y→	40									
	3 a	13									ϕ_1
	4 ↓	25	ϕ_1	z_1	z_1						
	5 cos	73	$\cos \phi_1$	"	"						
	6 ÷		"	r_1	"						
	7 2	02									
	8 .	21									
	9 5	05	I	"	"						
	a ±	35		$\tan \theta_1$							
	b ↓	25	$\tan \theta_1$	z_1							
	c ARC	72									
	d TAN	71	θ_1								

Title Program A Date page A2

Name

Step	Key	Code	x	y	z	f	e	d	c	b	a
2 0	X →	23									
1	b	14								θ_1	ϕ_1
2	sin	70	$\sin\theta_1$	z_1	z_1						
3	↑	27	"	$\sin\theta_1$	"						
4	1	01									
5	−	21									
6	3	03									
7	3	03									
8	3	03	n	$\sin\theta_1$	z_1						
9	÷	35		$\sin\theta_1'$	"						
a	↓	25	$\sin\theta_1'$		"						
b	Arc	72									
c	sin	70									
d	X →	23									
3 0	C	16							θ_1'	θ_1	ϕ_1
1	Stop	41	x_2'	x_2'	z_2'						
2	1	01									
3	6	06									
4	0	00									
5	0	00	1600	x_2'	z_2'						
6	−	34		$x_2' - 1600$							
7	.	21									
8	0	0									
9	0	0									
a	0	0									
b	3	3									
c	5	05									
d	5	05	.000355	"	"						

Title Program A Date page A3

Name

Step	Key	Code	x	y	z	f	e	d	c	b	a
4 0	X	36	.000355	x_2	z_2'				θ_1'	θ_1	ϕ_1
1	Roll↑	72	z_2'	.000355	x_2						
2	X	36	"	z_2	x_2						
3	↓	25	z_2	x_2	"						
4	↑	27	"	z_2	x_2						
5	Roll↑	31	"	x_2	z_2						
6	Polar	62	$\lvert r_2 \rvert$	ϕ_2	"						
7	y→	40									
8	d	17						ϕ_2	θ_1'	θ_1	ϕ_1
9	↓	25	ϕ_2	z_2	"						
a	cos	73	cos ϕ_2								
b	÷	35		r_2							
c	2	02									
d	.	21									
5 0	5	05	I	r_2	z_2						
1	÷	35		tan θ_2							
2	↓	25	tan θ_2	z_2	z_2						
3	Arc	72									
4	Tan	71	θ_2	"	"						
5	X→	23									
6	e	12					θ_2	ϕ_2	θ_1'	θ_1	ϕ_1
7	sin	70	sin θ_2								
8	↑	27		sin θ_2	z_2						
9	1	01									
a	·	21									
b	3	03									
c	3	03									
d	3	03	n	sin θ_2	z_2						

Title Program A Date page A4

Name

Step	Key	Code	x	y	z	f	e	d	c	b	a
6	0 ÷	35	n	$\sin\theta'_2$	z_2						
	1 ↓	25	$\sin\theta'_2$	z_2	"						
	2 Arc	72									
	3 Sin	70	θ'_2								
	4 X→	23									
	5 f	15				θ'_2	θ_2	ϕ_2	θ'_1	θ_1	ϕ_1
	6 End	46									
	7		To To Program B								

Title Program B Date page B1

Name

Step	Key	Code	x	y	z	f	e	d	c	b	a
0	0	1				θ_2'	θ_2	ϕ_2	θ_1'	θ_1	ϕ_1
	1	9									
	2	.									
	3	8	L_1								
	4	↑		L_1							
	5	b	θ_1								
	6	Tan	Tan θ_1								
	7	X		e_1							
	8	1									
	9	8									
	a	3	b								
	b	↑		b	e_1						
	c	c	θ_1'								
	d	Tan	Tan θ_1'								
1	0	X 36		e_2							
	1	↓ 25	e_2	e_1							
	2	+ 33		e'							
	3	a 13	ϕ_1								
	4	cos 73	cos ϕ_1								
	5	x 36		e							
	6	y→ 40				θ_2'	θ_2	ϕ_2	ϕ_1'	e	ϕ_1
	7	b 14									
	8	a 13	ϕ_1								
	9	cos 73	cos ϕ_1								
	a	↑ 27		cos ϕ_1	e						
	b	c 16	θ_1'								
	c	Tan 71	Tan θ_1'								
	d	X 36		Tan θ_1' cos ϕ_1							

Step	Key	Code	x	y	z	f	e	d	c	b	a
20	d	17	ϕ_2								
1	Tan	71	Tan ϕ_2								
2	Chg Sign	32	-Tan ϕ_2								
3	X	36		c							
4	y→	40									
5	c	16							c		
6	1	01									
7	7	07									
8	•	21									
9	5	05	L_2								
a	↑	27		L_2							
b	e	12	θ_2								
c	Tan	71	Tan θ_2								
d	x	36		f_1							
0	1	01									
1	8	00									
2	3	03	b								
3	↑	27		b	f_1						
4	f	15	θ_2'								
5	Tan	71	Tan θ_2'								
6	x	36		f_2	f_1						
7	+	25	f_2	f_1							
8	+	33		f'							
9	d	17	ϕ_2								
a	cos	73	cos ϕ_2								
b	X	36		f							
c	y→	40									
d	e	12					f				

Step		Key	Code	x	y	z	f	e	d	c	b	a
4	0	d	17	ϕ_2								
	1	cos	73	cos ϕ_2								
	2	↑	27		cos ϕ_2							
	3	f	15	θ'_2								
	4	Tan	71	Tan θ'_2								
	5	X	36		Tan θ'_2 Cos ϕ_2							
	6	a	13	ϕ_1								
	7	Tan	71	Tan ϕ_1								
	8	Chg Sign	32	-Tan ϕ_1								
	9	X	36		d							
	a	y→	40									
	b	f	15				d					
	c	Stop	41				d	f	ϕ_2	c	e	ϕ_1
	d	c	16	c								
5	0	↑	27		c							
	1	1	01	1								
	2	↑	27		1	c						
	3	f	15	d								
	4	÷	35		1/d							
	5	+	25	1/d	c							
	6	-	34		c - 1/d							
	7	y	24									
	8	b	14		e						c-1/d	
	9	e	12	f								
	a	↑	27		f	e						
	b	f	15	d	f	e						
	c	÷	35		f/d							
	d	+	25	f/d	e							

Title Program B Date page B4

Name

Step	Key	Code	x	y	z	f	e	d	c	b	a
6	0 -	34		e - f/d							
	1 b	14	c - 1/d								
	2	35		Z_2							
	3 Print	45									
	4 y→	40									
	5 b	14								Z_2	
	6 c	16	c	Z_2	e						
	7 X	36		cZ_2							
	8 +	25	dZ_2	e							
	9 -	34		Z_1							
	a Print	45									
	b a	13	ϕ_1								
	c Tan	71	Tan ϕ_1	Z_1							
	d X	36		Y							
	0 Print	45									
	1 d	17	ϕ_2								
	2 Tan	71	Tan ϕ_2								
	3 Roll↑	22	e	Tan θ_2	Y						
	4 b	14	c	Tan θ_2							
	5 X	36		X							
	6 Print	45									
	7 End	46									
	8		If Not Last Point Go To Program A								

Title Program C Date page C1

Name

Step	Key	Code	x	y	z	f	e	d	c	b	a
0	0	Clear 20									
	1	x→( ) 23									
	2	d 17									
	3	x→( ) 23									
	4	c 16									
	5	x→( ) 23									
	6	b 14									
	7	1 01									
	8	x→( ) 23									
	9	a 13									
	a	Stop 41	x_i	y_i	0						
	b	If Flag 43									
	c	3 03									
	d	7 07									
	0	Acct 60									
	1	↑ 27									
	2	x 36									
	3	x y 30									
	4	y 24									
	5	d 17									
	6	+ 33									
	7	y 24									
	8	d 17									
	9	+ 25									
	a	x 36									
	b	b 14									
	c	+ 33									
	d	y→( ) 40									

Title Program C

Date page C2

Name

Step	Key	Code	x	y	z	f	e	d	c	b	a
2	0 b	14									
	1 Roll↓	22									
	2 ↑	27									
	3 x	36									
	4 c	16									
	5 +	33									
	6 y→( )	40									
	7 c	16									
	8 a	13									
	9 ↑	27									
	a 1	01									
	b +	33									
	c y→( )	40									
	d a	13									
3	0 0	00									
	1 Roll↓	31									
	2 x y	30									
	3 ↓	25									
	4 Go To	44									
	5 0	00									
	6 a	13									
	7 a	13									
	8 ↑	27									
	9 1	01									
	a -	34									
	b ↓	25									
	c x→( )	23									
	d a	13									

Title Program C Date page C3

Name

Step	Key	Code	x	y	z	f	e	d	c	b	a
40	e	12									
1	↑	27									
2	a	13									
3	÷	35									
4	y	24									
5	f	15									
6	÷	35									
7	y	40									
8	e	12									
9	x	36									
a	e	12									
b	x	36									
c	d	17									
d	x y	30									
0	-	34									
1	y→( )	40									
2	d	17									
3	c	16									
4	↑	27									
5	f	15									
6	↑	27									
7	x	36									
8	a	13									
9	x	36									
a	+	25									
b	-	34									
c	y→( )	40									
d	c	16									

Title Program C Date page C4

Name

Step		Key	Code	x	y	z	f	e	d	c	b	a
6	0	b	14									
	1	↑	27									
	2	f	15									
	3	↑	27									
	4	3	12									
	5	x	36									
	6	a	13									
	7	x	36									
	8	↓	25									
	9	-	34									
	a	d	17									
	b	↑	27									
	c	↓	25									
	d	x	76									
7	0	÷	35									
	1	c	16									
	2	x	76									
	3	÷	35									
	4	d	17									
	5	Roll↓	22									
	6	x y	30									
	7	÷	35									
	8	y	24									
	9	e	12									
	a	e	12									
	b	x	36									
	c	f	15									
	d	x y	30									

Title Program C Date page C5

Name

Step	Key	Code	x	y	z	f	e	d	c	b	a
8	0	- 34									
1	A	12									
2	End	46	m	b	R						

BIBLIOGRAPHY

1. Bacon, D. L. and Reid, E. G., "Resistance of Spheres in Wind Tunnels and in Air," National Advisory Committee for Aeronautics Report No. 185 (1924).

2. Batchelor, G. K., Fluid Dynamics, Cambridge University Press, New York (1967).

3. Barker, D. H., "Effects of Shape and Density on the Free Settling Rates of Particles at High Reynolds Numbers," Ph. D. Thesis, University of Utah, Salt Lake City, Utah (1951).

4. Carey, W. W. and Turian, R. M., "Settling of Spheres in Drag Reducing Polymers Solutions," Industrial and Engineering Chemistry Fundamentals, vol. 9-1: 187 (1970).

5. Chenard, J. H., "Drag of Spheres in Dilute Aqueous Solutions of Poly(ethylene oxide) within the Region of the Critical Reynolds Number," M. S. Thesis, Naval Postgraduate School, Monterey, California (1967).

6. Fidleris, V. and Whitmore, R. L., "Experimental Determination of the Wall Effects for Spheres Falling Axially in Cylindrical Vessels," British Journal of Applied Physics, vol. 12: 490 (1916).

7. Flachsbart, O., "Neuere Untersuchungen uber den Luftwiderstand von Kugelin," Phys. Z., vol. 28: 461 (1927).

8. Hampton, L. D., and McKinney, C. M., "Experimental Study of the Scattering of Acoustic Energy from Solid Metal Spheres in Water," Journal of the Acoustical Society of America, vol. 33-5: 664 (1961).

9. Goldstein, S., Modern Developments in Fluid Dynamics Vol. II, Oxford University Press, London (1938).

10. Hayes, M. F., "Drag Coefficients of Spheres Falling in Dilute Aqueous Solutions of Long-Chain Macromolecules," M.S. Thesis, Naval Postgraduate School, Monterey, California (1966).

11. Hoerner, S. F., "Influence of Reynolds Number, Turbulence and Surface Roughness on Spheres," National Advisory Committee for Aeronautics Technical Memorandum No. 777 (1935).

12. Hoerner, S. F., Fluid Dynamic Drag, Published by author, Midland Park, New Jersey (1965).

13. Hoyt, J. W. and Fabula, A. G., "The Effect of Additives of Fluid Friction," Fifth Symposium on Naval Hydrodynamics, Bergin, Norway (1959).

14. Jacobs, E. N., "Sphere Drag Tests in the Variable Density Wind Tunnel," National Advisory Committee for Aeronautics Report No. 312 (1929).

15. Kinnier, J. W., "A Correlation Between Friction Reduction and Molecular Size for the Flow of Dilute Aqueous Polyethylene-oxide Solutions in Pipes," Ph. D. Thesis, Naval Postgraduate School, Monterey, California (1970).

16. Lang, T. G. and Patrick, H. V. L., "Drag of Blunt Bodies in Polymer Solutions," Naval Ordnance Test Station TP 4379, China Lake, California (1967).

17. Lunnon, R. G., "Fluid Resistance to Moving Spheres," Royal Society of London, Proceedings, vol. 118A: 680 (1928).

18. Lunnon, R. G., "Fluid Resistance to Moving Spheres," Royal Society of London, Proceedings, vol. 110A: 302 (1926).

19. Magarney, R. H. and MacLatchy, C. S., "Vortices in Sphere Wakes," Canadian Journal of Physics, vol. 43-9: 1649 (1965).

20. McNown, J. S., Lee, H. M., McPherson, M. B., and Engez, S. M., "Influence of Boundary Proximity on the Drag of Spheres," Proceedings of the Seventh International Congress of Applied Mechanics (1948).

21. Millikan, C. B. and Klein, A. L., "Effect of Turbulence, "Aircraft Engineering, vol. 5: 169 (1933).

22. Odar, F., "Verification of the Proposed Equation for Calculation of the Forces on a Sphere Accelerating in a Viscous Fluid," U. S. A. Cold Regions Research and Engineering Laboratory Research Report 190

23. Odar, F. and Hamilton, W. S., "Forces on a Sphere Accelerating in a Viscous Fluid," Journal of Fluid Mechanics, vol. 18-2: 302 (1963).

24. Pasternak, I. S., "Turbulent Convective Heat and Mass Transfer from Stationary and Accelerating Particles," Ph. D. Thesis, McGill University, Montreal, Canada (1959).

25. Pitkin, E. T., "Determination of Flight Speeds and Drag Coefficients from Time and Distance Measurements," Journal Spacecraft, vol. 8-5: 1001 (1968).

26. Roshko, A., "Experiments on the Flow Past a Circular Cylinder at Very High Reynolds Numbers," Journal of Fluid Mechanics, vol. 10: 345 (1961).

27. Sanders, J. V., "Drag Coefficients of Spheres in Poly(ethylene oxide) Solutions," International Shipbuilding Progress, vol. 14-152: 140 (1967).

28. Schlichting, H., Boundary Layer Theory, 4th ed., McGraw-Hill Book Company, Inc., New York (1960).

29. Taneda, S., "Negative Magnus Effect," Research Institute for Applied Mechanics, vol. 5-20: 123, Kyushu University, Fukuoka, Japan (1957).

30. Toms, B. A., "Some Observations on the Flow of Linear Polymer Solutions Through Straight Tubes at Large Reynolds Numbers," Proceedings of the First International Congress on Rheology, North Holland Publishing Company, Amsterdam (1949).

31. Torobin, L. B. and Gauvin, W. H., "Fundamental Aspects of Solids-Gas Flow, Part I: Introductory Concepts and Idealized Sphere Motion in Viscous Regime," Canadian Journal of Chemical Engineering, vol. 37:129 (1959).

32. Torobin, L. B. and Gauvin, W. H., "Fundamental Aspects of Solids-Gas Flow, Part II: The Sphere Wake in Steady Laminar Fluids," Canadian Journal of Chemical Engineering, vol. 37: 167 (1959).

33. Torobin, L. U. and Gauvin, W. H., "Fundamental Aspects of Solids-Gas Flow, Part III: Accelerated Motion of a Particle in a Fluid," Canadian Journal of Chemical Engineering, vol. 37: 224 (1959).

34. Torobin, L. B. and Gauvin, W. H., "Fundamental Aspects of Solids-Gas Flow, Part IV: Effects of Particle Rotation, Roughness, and Shape," Canadian Journal of Chemical Engineering, vol. 38: 142 (1960).

35. Torobin, L. B. and Gauvin, W. H., "Fundamental Aspects of Solids-Gas Flow, Part V: Effects of Fluid Turbulence on the Particle Drag Coefficient," Canadian Journal of Chemical Engineering, vol. 38: 189 (1960).

36. Wieselsberger, C., "Uber den Luftwderstand bei Gleichzeitiger Rotation des Versuchshorpers," Phys. Z. vol. 28: 84 (1927).

37. Woolery, E. F., "Drag of Free Falling Spheres in Dilute Aqueous Solutions of Poly(ethylene oxide) for Reynolds Number Above Critical Value," M.S. Thesis, Naval Postgraduate School, Monterey, California (1968).

INITIAL DISTRIBUTION LIST

		No. Copies
1.	Defense Documentation Center Cameron Station Alexandria, Virginia 22314	2
2.	Library, Code 0212 Naval Postgraduate School Monterey, California 93940	2
3.	Assoc. Professor J. V. Sanders, Code 61Sd Department of Physics Naval Postgraduate School Monterey, California 93940	3
4.	LT George F. Nolan, USN 1326 W. 27th Street San Pedro, California 90731	1
5.	Dr. J. W. Hoyt Naval Undersea Research & Development Center 3202 E. Foothill Blvd. Pasadena, California 91107	1
6.	Dr. A. G. Fabula Naval Undersea Research & Development Center 3202 E. Foothill Blvd. Pasadena, California 91107	1
7.	Professor G. W. Rodeback, Code 61Rk Department of Physics Naval Postgraduate School Monterey, California 93940	1

UNCLASSIFIED
Security Classification

DOCUMENT CONTROL DATA - R & D

(Security classification of title, body of abstract and indexing annotation must be entered when the overall report is classified)

1 ORIGINATING ACTIVITY (Corporate author)
Naval Postgraduate School
Monterey, California 93940

2a. REPORT SECURITY CLASSIFICATION
Unclassified

2b. GROUP

3 REPORT TITLE
Drag of Free-Falling Spheres in Water for Reynolds Numbers Near Critical

4 DESCRIPTIVE NOTES (Type of report and, inclusive dates)
Master's Thesis, September 1970

5. AUTHOR(S) (First name, middle initial, last name)
George F. Nolan

6. REPORT DATE	7a. TOTAL NO. OF PAGES	7b. NO. OF REFS
September 1970	88	37

8a. CONTRACT OR GRANT NO.	9a. ORIGINATOR'S REPORT NUMBER(S)
b. PROJECT NO.	
c.	9b. OTHER REPORT NO(S) (Any other numbers that may be assigned this report)
d.	

10. DISTRIBUTION STATEMENT
This document has been approved for public release and sale; its distribution is unlimited.

11. SUPPLEMENTARY NOTES	12. SPONSORING MILITARY ACTIVITY
	Naval Postgraduate School Monterey, California 93940

13. ABSTRACT

Drag coefficients of free-falling spheres in water were determined in a 12-ft diameter tank. Nine spheres with weights ranging from 361 grams to 4587 grams were released from rest and their speeds measured 19.5 feet below the release point using orthonormal cinematography. The region of both sides of the critical Reynolds number was covered with Reynolds numbers ranging from 10^5 to 7×10^5. Spheres with Reynolds numbers less than the critical value displayed little scatter in their terminal velocities. The same was true for the heaviest sphere. However, spheres with Reynolds number immediately above the critical value frequently deviated from the normal trajectory and their speeds showed scatter as great as 20%. A plot of drag coefficient versus Reynolds number shows that free-falling spheres essentially conform to the wind tunnel results; the critical Reynolds number is unchanged and the drag coefficients differ no more than 20%, always being higher for the free-fall case.

DD FORM 1 NOV 65 1473 (PAGE 1)
S/N 0101-807-6811

UNCLASSIFIED
Security Classification

A-31408

KEY WORDS	LINK A		LINK B		LINK C	
	ROLE	WT	ROLE	WT	ROLE	WT
Sphere						
Drag Coefficients						
Reynolds number						
Free-fall						
Critical Region						
Water						
Orthonormal cinematography						

124309

Thesis
N77
c.1

Nolan
Drag of free-falling spheres in water for Reynolds numbers near critical.